IAEA TECDOC SERIES

IAEA-TECDOC-1931

IAEA-TECDOC-1931

An Introduction to Practical Industrial Tomography Techniques for Non-destructive Testing (NDT)

IAEA
International Atomic Energy Agency

AN INTRODUCTION TO PRACTICAL INDUSTRIAL TOMOGRAPHY TECHNIQUES FOR NON-DESTRUCTIVE TESTING (NDT)

The following States are Members of the International Atomic Energy Agency:

AFGHANISTAN
ALBANIA
ALGERIA
ANGOLA
ANTIGUA AND BARBUDA
ARGENTINA
ARMENIA
AUSTRALIA
AUSTRIA
AZERBAIJAN
BAHAMAS
BAHRAIN
BANGLADESH
BARBADOS
BELARUS
BELGIUM
BELIZE
BENIN
BOLIVIA, PLURINATIONAL STATE OF
BOSNIA AND HERZEGOVINA
BOTSWANA
BRAZIL
BRUNEI DARUSSALAM
BULGARIA
BURKINA FASO
BURUNDI
CAMBODIA
CAMEROON
CANADA
CENTRAL AFRICAN REPUBLIC
CHAD
CHILE
CHINA
COLOMBIA
COMOROS
CONGO
COSTA RICA
CÔTE D'IVOIRE
CROATIA
CUBA
CYPRUS
CZECH REPUBLIC
DEMOCRATIC REPUBLIC OF THE CONGO
DENMARK
DJIBOUTI
DOMINICA
DOMINICAN REPUBLIC
ECUADOR
EGYPT
EL SALVADOR
ERITREA
ESTONIA
ESWATINI
ETHIOPIA
FIJI
FINLAND
FRANCE
GABON
GEORGIA
GERMANY
GHANA
GREECE
GRENADA
GUATEMALA
GUYANA
HAITI
HOLY SEE
HONDURAS
HUNGARY
ICELAND
INDIA
INDONESIA
IRAN, ISLAMIC REPUBLIC OF
IRAQ
IRELAND
ISRAEL
ITALY
JAMAICA
JAPAN
JORDAN
KAZAKHSTAN
KENYA
KOREA, REPUBLIC OF
KUWAIT
KYRGYZSTAN
LAO PEOPLE'S DEMOCRATIC REPUBLIC
LATVIA
LEBANON
LESOTHO
LIBERIA
LIBYA
LIECHTENSTEIN
LITHUANIA
LUXEMBOURG
MADAGASCAR
MALAWI
MALAYSIA
MALI
MALTA
MARSHALL ISLANDS
MAURITANIA
MAURITIUS
MEXICO
MONACO
MONGOLIA
MONTENEGRO
MOROCCO
MOZAMBIQUE
MYANMAR
NAMIBIA
NEPAL
NETHERLANDS
NEW ZEALAND
NICARAGUA
NIGER
NIGERIA
NORTH MACEDONIA
NORWAY
OMAN
PAKISTAN
PALAU
PANAMA
PAPUA NEW GUINEA
PARAGUAY
PERU
PHILIPPINES
POLAND
PORTUGAL
QATAR
REPUBLIC OF MOLDOVA
ROMANIA
RUSSIAN FEDERATION
RWANDA
SAINT LUCIA
SAINT VINCENT AND THE GRENADINES
SAN MARINO
SAUDI ARABIA
SENEGAL
SERBIA
SEYCHELLES
SIERRA LEONE
SINGAPORE
SLOVAKIA
SLOVENIA
SOUTH AFRICA
SPAIN
SRI LANKA
SUDAN
SWEDEN
SWITZERLAND
SYRIAN ARAB REPUBLIC
TAJIKISTAN
THAILAND
TOGO
TRINIDAD AND TOBAGO
TUNISIA
TURKEY
TURKMENISTAN
UGANDA
UKRAINE
UNITED ARAB EMIRATES
UNITED KINGDOM OF GREAT BRITAIN AND NORTHERN IRELAND
UNITED REPUBLIC OF TANZANIA
UNITED STATES OF AMERICA
URUGUAY
UZBEKISTAN
VANUATU
VENEZUELA, BOLIVARIAN REPUBLIC OF
VIET NAM
YEMEN
ZAMBIA
ZIMBABWE

The Agency's Statute was approved on 23 October 1956 by the Conference on the Statute of the IAEA held at United Nations Headquarters, New York; it entered into force on 29 July 1957. The Headquarters of the Agency are situated in Vienna. Its principal objective is "to accelerate and enlarge the contribution of atomic energy to peace, health and prosperity throughout the world''.

IAEA-TECDOC-1931

AN INTRODUCTION TO PRACTICAL INDUSTRIAL TOMOGRAPHY TECHNIQUES FOR NON-DESTRUCTIVE TESTING (NDT)

INTERNATIONAL ATOMIC ENERGY AGENCY
VIENNA, 2020

COPYRIGHT NOTICE

For further information on this publication, please contact:

Radioisotope Products and Radiation Technology Section
International Atomic Energy Agency
Vienna International Centre
PO Box 100
1400 Vienna, Austria
Email: Official.Mail@iaea.org

Printed by the IAEA in Austria
December 2020

IAEA Library Cataloguing in Publication Data

Names: International Atomic Energy Agency.
Title: An introduction to practical industrial tomography techniques for non-destructive testing (NDT) / International Atomic Energy Agency.
Description: Vienna : International Atomic Energy Agency, 2020. | Series: IAEA TECDOC series, ISSN 1011–4289 ; no. 1931 | Includes bibliographical references.
Identifiers: IAEAL 20-01358 | ISBN 978–92–0–120920–7 (paperback : alk. paper) | ISBN 978–92–0–121020–3 (pdf)
Subjects: LCSH: Nondestructive testing. | Tomography. | Imaging systems.

FOREWORD

The IAEA promotes industrial applications of radiation technology, including advanced non-destructive testing (NDT) and non-destructive evaluation (NDE), through various coordinated research projects and regional and country level technical cooperation projects. The advanced radioisotope and radiation based NDT and NDE technologies include computed radiography (CR), digital industrial radiography (DIR) and industrial computed tomography (ICT).

CR and DIR equipment is now commercially available in many companies. As it has become more standardized, compact and robust, and as its cost–benefit ratio has improved, such equipment has become more widely accessible, and many NDT centres and practitioners are now able to use CR and DIR for routine NDT practice.

In contrast, the use of ICT for advanced industrial NDE is still relatively limited. One reason is that ICT is a very complex area of technology encompassing nuclear radiation detectors, mechanical engineering, computational mathematics and radiation physics. Moreover, as an imaging modality, computed tomography is entirely different from conventional projection radiography, and the specific requirements for NDE may make it prohibitively expensive for the average user at present.

As a first step toward introducing this technology more widely, participants in IAEA projects have begun setting up ICT imaging systems in nuclear radiation laboratories using readily available subsystems. Such introductory level systems can then be used for training and education purposes in Member States, and the expertise gained can later be used in setting up large, complex industrial tomography facilities.

The present publication is aimed at helping participating organizations in Member States and those the NDT community who are practising conventional radiography techniques to better understand the intricacies of computed industrial tomography. In particular, it provides information on various practical issues and problems relating to setting up a gamma computed tomography for NDE imaging using these simple configurations.

The IAEA officer responsible for this publication was P. Brisset of the Division of Physical and Chemical Sciences.

EDITORIAL NOTE

This publication has been prepared from the original material as submitted by the contributors and has not been edited by the editorial staff of the IAEA. The views expressed remain the responsibility of the contributors and do not necessarily represent the views of the IAEA or its Member States.

Neither the IAEA nor its Member States assume any responsibility for consequences which may arise from the use of this publication. This publication does not address questions of responsibility, legal or otherwise, for acts or omissions on the part of any person.

The use of particular designations of countries or territories does not imply any judgement by the publisher, the IAEA, as to the legal status of such countries or territories, of their authorities and institutions or of the delimitation of their boundaries.

The mention of names of specific companies or products (whether or not indicated as registered) does not imply any intention to infringe proprietary rights, nor should it be construed as an endorsement or recommendation on the part of the IAEA.

The authors are responsible for having obtained the necessary permission for the IAEA to reproduce, translate or use material from sources already protected by copyrights.

The IAEA has no responsibility for the persistence or accuracy of URLs for external or third party Internet web sites referred to in this publication and does not guarantee that any content on such web sites is, or will remain, accurate or appropriate.

Contents

1. INTRODUCTION

The process of Non-Destructive Testing (NDT) or Examination (NDE) determines the existence of flaws, discontinuities, leaks, contamination, thermal anomalies, or imperfections in materials, components or assemblies without impairing the integrity or function of the inspected component. NDE is also utilized for real-time monitoring during manufacturing, inspection of assemblies for tolerances, alignment, and periodic in-service monitoring of flaw/damage growth in order to determine the maintenance requirements and to assure the reliability and continued safe operation of the part. Conventional Industrial Radiography is an adaptation of the principle of latent image formation on photographic medium by gamma rays or X rays for non-medical applications. Film-based gamma ray and X ray radiography for examination of industrial specimen has been in practice for many decades and it has become an indispensable tool for industrial quality control in production, maintenance and in-service inspection. A γ ray or an X ray radiograph unlike a picture is not so easily interpreted because it is produced in a way that is not directly understood. If the structures in a radiograph are to be analysed, the interpretation has to be complemented by a conscious logical process based on the understanding of the production of the radiograph. In general, three reasons may be attributed to the efforts for the development of other imaging methods: (a) a large proportion of the available information is lost when one superimposes three-dimensional information onto a two-dimensional detector; (b) the detector medium is unable to record or display minute transmitted radiation differences and (c) a large percentage of the radiation detected is scattered from the object itself. Tomography refers to the synthesis of sectional images or slices from external measurements of a spatially varying function. As it is generally seen, tomography is often perceived as an imaging tool for medical examination purposes. It must be emphasised, however, that the concept of tomography and its non-invasive way of imaging are not restricted to the medical field. Tomography has been developing, mainly over the last two decades or so, into a reliable tool for imaging numerous industrial applications [1]. Non-invasive techniques - those that do not, as a result of the inspection method, damage the object's integrity or health - are all classified under the heading of non-*destructive evaluation* (NDE)**.**

Electronic imaging devices for gamma and X ray based radiography testing (RT) have shown a remarkable presence during the last two decades due to their technical adaptability to existing inspection systems and easy availability of different configurations to suit a variety of applications. Today one can find both analog and digital imaging systems like tube-type fluoroscopy devices, solid-state linear detector arrays (LDA) and two-dimensional detector arrays like flat panel detectors (FPD). These devices can be adapted to suit a variety of imaging requirement like Digital Industrial Radiography (DIR) operating in online and/or real-time mode and the fast-emerging Industrial Computed Tomography (ICT) imaging for non-medical applications. A typical DIR and ICT system may be very compact and modular for low-energy applications. However, dedicated DIR and ICT systems designed and developed for specific requirements and making use of high-energy X rays may be a fixed installation. Industrial Computed Tomography (ICT) utilizing penetrating nature of ionizing radiation is a highly complex computational imaging technology. However, in its simplest form, a typical laboratory-scale transmission-type ICT based on gamma rays emanating from radioisotope sources can be setup using a single nucleonic detector and other devices.

1.1. SCOPE OF THE GUIDEBOOK

The scope of this technical manual / guidebook is limited to:
(i) a brief and simplified overview of theoretical background of industrial computed tomography (ICT) imaging modality; (ii) practical aspects and to-do steps for configuring a single detector based gamma transmission tomography laboratory set-up; (iii) some basic system evaluation techniques; (iv) steps involved in setting up a typical linear detector array (LDA) based axial computed tomography facility; (vi) a brief outline of a typical 2D digital detector array (DDA) based tomography configuration using constant potential (CP) X ray source in addition to some discussion on Standards and Guidelines and availability of ICT software.

The guidebook does not recommend any specific mechanical manipulator, detector system or hardware control software as these sub-systems are manufacturer-specific and vary a lot. This is also not in the scope of providing a treatise on calibration and optimization of LDA and DDA or recommending any specific software system either for data acquisition, machine control, image reconstruction or visualization and analysis.
The sketches, photographs and schematics referred to in this technical manual is for visual assistance in explaining concepts and exclusively for teaching and training purpose only.

1.2. ADVISORY ON RADIATION SAFETY ISSUES

It is beyond the scope of this technical guidebook to address the radiological safety issues associated with any possible experiment(s) being attempted by the interested readers in their laboratories using any type of ionizing radiation. It is strongly advised that all facilities and imaging laboratories have the necessary radiation safety devices installed and all such radiation imaging facilities adhere to the existing national and international radiation safety regulations in the Member State.
For details on specific precautions and safety measures while dealing with radioisotope and X ray based industrial exposure devices please refer to IAEA Safety Standards Series No. SSG-11, Radiation Safety in Industrial Radiography (2011).

1.3. PROJECTION RADIOGRAPHY AND COMPUTED TOMOGRAPHY

Sealed radioisotope source based γ rays as well as machine based X rays are electromagnetic radiations and have considerable penetrating power in almost all solids and fluid materials of scientific and engineering interest. The penetrating nature of γ rays and X rays has been made use in visualising internal details of an object. When a beam of such a radiation is allowed to fall on any material substance, interaction takes place between radiation and matter, and part of the energy of the probing radiation is removed from the beam either by absorption or by scattering. This imaging process produces a two-dimensional presentation of a three-dimensional object. The relative intensities in this representation convey information about the radiological thickness (absorptions) of various structures whereas the spatial distribution of the intensities conveys information about the shapes [2].

An image in its most general term may be defined as a function of spatial or perhaps temporal variables. The process of image formation requires interaction of some kind of radiation as a

probing beam and detecting and recording the emergent radiation from the interacting medium. In almost all cases, an image virtually approximates the object and the exact reproduction is never possible on account of the statistical nature of the processes involved.

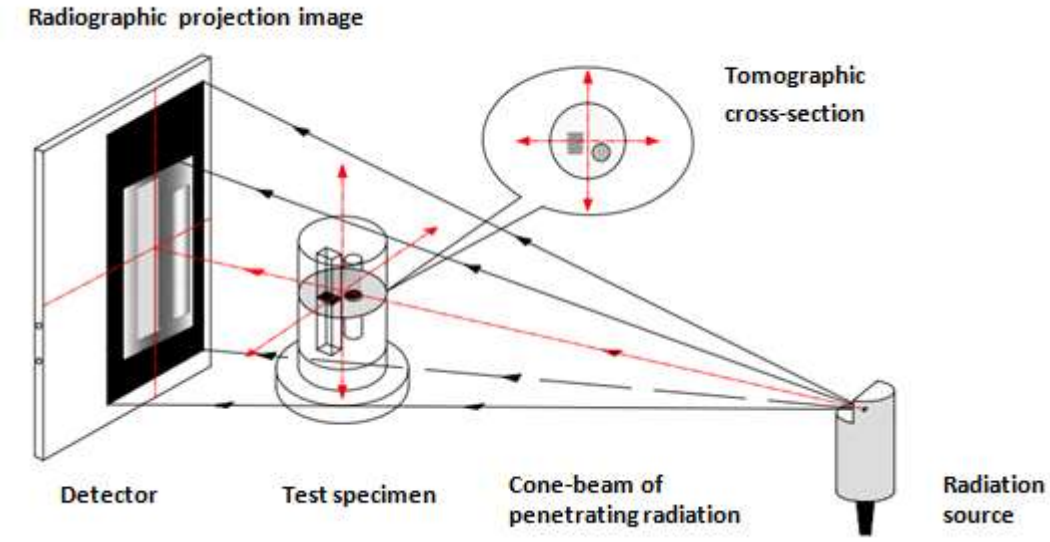

FIG. 1. Projection radiography and tomography

Figure 1 illustrates the fundamental difference in the projection radiography and a typical sectional tomography imaging plane through a three-dimensional object. In radiography, the image formation is a direct process based on preferential absorption of penetrating radiation by the matter. The visualization of a thin cross-sectional plane at any angle through the object is in general an indirect technique. Computed tomography (CT) is the general term used to define a class of reconstructive sectional imaging methods and specifically in X-rays and gamma-ray based transmission-type computed tomography; the photons are restricted to enter the other planes of the object under examination. If a sufficient number of views or projections are taken, the distribution of approximate linear attenuation coefficients within the layer may be determined. The fundamental task of an industrial transmission-type tomography system is to make an extremely large number of highly accurate measurements of gamma ray or X ray transmission through an object in a precisely controlled geometry. The next step is to computationally process this data to recover an approximate distribution of linear attenuation coefficients (computed tomography) at the effective energy of the probing radiation, which can be used to display the tomographic cross-section as an image. The reconstruction problem is the problem of inverting a finite number of projections at different angles to yield an estimate of the object function.

1.4.ICT AS AN ADVANCED NDE TECHNOLOGY

The industrial applications of tomography are still picking up primarily because one set of specifications does not cater to all problem areas. As a result, it appears that no universal industrial CT system has ever been built or standardised. There is in general, no concern for radiation exposure to the specimen under scanning which is in sharp contrast to the stringent regulations for medical CT systems. In addition, a broad class of industrial specimens do not have any inherent motion. Computed tomography as such, is a complex mathematical procedure involving a number of parameters. The specific advantages of the tomographic imaging can be summarised as follows:

- The technique provides a map of radiation absorption coefficient for each pixel from the tomogram, which leads to high-accuracy detection of small variations (faults and flows) in the investigated object;
- The dimension of the flaw is absolute (not projection or equivalent dimension), blurred only by noise and scattering effects, and a three-dimensional tomogram shows the real shape and dimension of object's constituents (absolute maximum length of a flaw, for example).

A fundamental task of CT systems is to make an extremely large number of highly accurate measurements of gamma ray or X ray transmission through an object in a precisely controlled geometry. CT information is derived from a large number of systematic observations at different viewing angles, and an image matrix is then numerically reconstructed. Thus, in principle, by using CT one can in effect, slice open the test article, examine its internal features record the different attenuations, perform dimensional inspections and identify any material or structural anomalies that may exist. In addition, by stacking and comparing adjacent CT slices of a test article, a three-dimensional image of the test article can be constructed. However, slight variations in different sub-system's characteristics may give rise to unique problems and necessitate a thorough study. It may also ask for a careful solution to the artefacts.

The three important scanning geometries from the point of view of industrial applications are as follows:
(i) Parallel-beam geometry is technically the simplest and the easiest one to understand the important ICT principles. Multiple measurements of transmitted radiation intensities are obtained using a single highly collimated gamma ray or X ray pencil beam and a detector. The beam is translated in a linear motion to obtain a projection profile.
(ii) A fan beam of generally X rays illuminates a large number of detector elements arranged along an arc (equiangular) or a line (collinear). The object is fully covered by the fan beam. An object rotation by 360^0 and no translation motion is used to generate projection data. As a result, these rotate-only motions acquire projection data for a single image. The object can have either start-stop motion or continuous motion.
(iii) A natural extension of this geometry is to employ a two-dimensional array detector and a cone-beam of radiation such that multiple projection lines can be acquired simultaneously, or volume reconstruction can be carried out [3].

There may however be different scanning mechanisms also based on selected reconstruction algorithms.

1.5.TRANSMISSION TYPE ICT USING GAMMA RAYS AND X RAYS

Computed tomography in general and industrial computed tomography in particular is the science of recovering an estimate of the internal structure of an object from a systematic non-destructive interrogation of some aspect of its physical properties. In gamma ray and X ray industrial CT imaging operating in transmission mode, the probing radiation source is generally a sealed radioisotope or a machine-based (constant-potential) industrial X ray tube. The transmitted radiation through the object can be simply measured using a single detector, a line array of detectors or a planar detector array depending upon the operational configuration. There may be other sub-systems e.g., mechanical manipulators in addition to software systems which would be required for specimen motion, data acquisition and image reconstruction.

The problem is manageable in a more general way by limiting the task to a determination of a single image plane through the object. In its basic form, the whole imaging sequence consists of measuring a complete set of line integrals involving the physical parameter of interest over the designated cross-section and then using some type of computational algorithm to recover an estimate of the spatial variation of the parameter over the desired slice. No universal industrial CT instrument exists because of variability in the size and composition of the object, scanning speed, resolution and cost etc. One of the limitations of the single detector configuration is the long scanning times. The scanning time is the total time taken by the mechanical movements as well as electronic data acquisition. As there is only one pencil beam, which is used for the complete scanning sequence, the scanning time becomes overtly long even for a fairly strong source activity. However, this alleviates some of the problems associated with multiple detectors. If scanning time is not a constraint, a single source-detector configuration provides possibly the best-reconstructed image when a monochromatic gamma ray source is used. This is for the fundamental reason that all the measurements of line integrals are carried out with the same device.

However, when many cross-sectional slices or volumetric data are required in a short time, using multiple detectors and different scanning sequences can shorten scanning time. Industrial CT imaging systems are often developed to have the object perform most or all of the motion sequences with the source and detector assemblies being stationary – exactly the opposite of the scheme used in medical systems. Industrial computed tomography, being an interdisciplinary subject encompasses radiation physics, mathematical sciences, and electronics and computer science.

2. THEORETICAL ASPECTS OF TRANSMISSION TYPE ICT

2.1.ATTENUATION OF GAMMA RAYS AND X RAYS

A brief introduction of the evolution of tomographic imaging has been covered in Chapter 1. This chapter will focus on the theoretical and mathematical aspects of the problem of image reconstruction from projections. In tomographic imaging, the fact that different kinds of material attenuate gamma rays and X rays unequally is utilized.

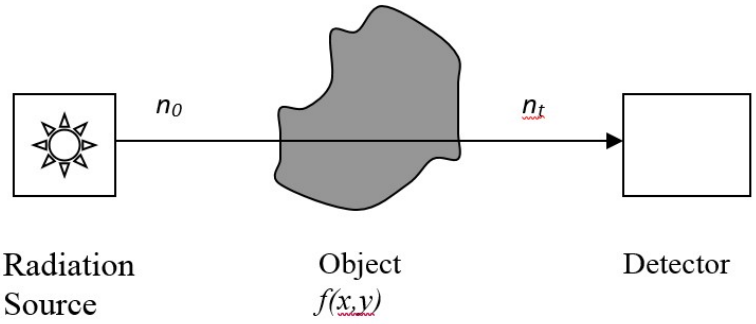

FIG. 2. Attenuation of penetrating radiation in matter

As shown in the figure 2, let n_0 and n_t be the intensities of the radiation beam incident on and transmitted through an object respectively. The object is characterized by a two-dimensional function *f(x,y)*. In the case of transmission computed tomography, *f(x,y)* represents the distribution of linear attenuation coefficients across the object cross-section. The relation between the intensities n_0 and n_t, in case of an idealized parallel beam configuration is described by

$$n_t = n_0 e^{-\int_l f(x,y)dl} \tag{1}$$

The logarithmic attenuation for each measurement, assuming monochromatic radiation, is given by Beer's Law.

$$-\log_e\left(n_t / n_0\right) = \int_l f(x,y).dl \tag{2}$$

The integral is over the complete length *l* along the beam path inside the object.

Primary measurements in the form of *line-integrals* are the basis for all transform-based tomography image reconstruction techniques. However, in a practical case, use of polychromatic radiation beam like bremsstrahlung X rays, detector sensitivity, loss of collimation and measurement errors change (2) to an approximation.

The ray-sum or line-integral for a monochromatic beam of energy E_0 will be represented in terms of the linear attenuation coefficients specifically by

$$-\log_e\left(n_t / n_0\right) = \int_l \mu(x,y,E_0).dl \tag{3}$$

The coordinate system as defined in figure 3 is normally used to describe projections. A *projection* is formed by combining a set of line integrals as defined by (2).

2.2.BASICS OF ICT IMAGE RECONSTRUCTION

2.2.1. Radon transform

The Radon transform $\Re f(t,\phi)$, or the *projection* $P_\phi(t)$, of an object *f(x,y)* is the line-integrals through the object in all possible directions. This means, a single Radon value is the integral of all points along a line with angle ϕ and perpendicular distance *t* from the origin. The Radon transform can be written as

$$P_\phi(t) = \Re f(t,\phi) = \int_{-\infty}^{\infty}\int_{-\infty}^{\infty} f(x,y)\delta(x\cos\phi + y\sin\phi - t)dxdy \qquad (4)$$

2.2.2. Fourier slice theorem

An important relationship between the Radon transform and the Fourier transform is the Fourier slice theorem.

The Fourier slice theorem states that the one-dimensional Fourier transform of the Radon transform along a radial line is identical to the same line in the two-dimensional Fourier transform of the object.

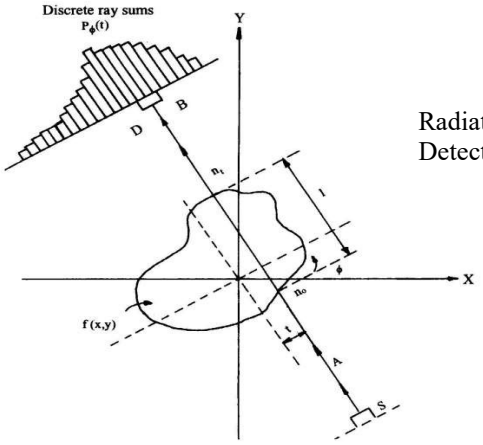

S: Radiation source, D: Detector

FIG. 3. Coordinate system to define projections

The two-dimensional Fourier transform of the object function *f(x,y)* is defined as

$$F(u,v) = \int_{-\infty}^{\infty}\int_{-\infty}^{\infty} f(x,y)\exp\left[-j2\pi(ux+vy)\right]dxdy \qquad (5)$$

Similarly, we can define the Fourier transform of a projection $P_\phi(t)$ at an angle ϕ as

$$S_\phi(w) = \int_{-\infty}^{\infty} P_\phi(t)\exp(-j2\pi wt)dt \qquad (6)$$

Following the analytical proof by Kak [4], it can be shown that

$$F(u,0) = S_{\phi=0}(u) \tag{7}$$

This is the simplest form of Fourier slice theorem for a projection at $\phi=0$. The Fourier slice theorem can be diagrammatically explained as shown in figure 4.

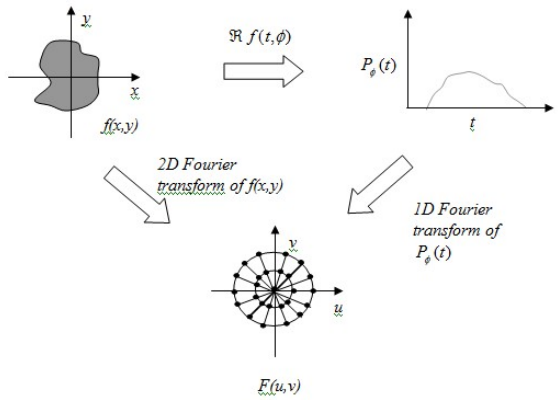

FIG. 4. The Fourier slice theorem

2.2.3. Reconstruction algorithms

The tomographic image reconstruction algorithms can be mainly divided into two groups: transform methods and series expansion methods irrespective of the geometry of data collection. Transform methods are fundamentally based on an inversion formula, which recovers f from its Radon, transform $\Re f$. Representing the inverse transform by the operator $\Re^{-1}$ gives

$$f(t,\phi) = \Re^{-1}\{\Re f(t,\phi)\} \tag{8}$$

Series expansion methods are based on the assumption that *f* can be discretely represented by an expansion of basic functions; then the reconstruction problem is reduced to the matrix problem of estimating the coefficients of the expansion [5].

2.3.PARALLEL-BEAM TOMOGRAPHY RECONSTRUCTION ALGORITHM

In parallel-beam industrial computed tomography, projection data or specifically the ray integrals are measured along parallel lines through the object. The radiation sources used in such experiments are generally a point source due to other considerations like geometrical unsharpness and blurring. This requires at least one detector and one source aligned on the same line, which sweeps through the object. Filtered back projection is one of the most frequently used reconstruction methods for two-dimensional tomographic imaging. The quality of reconstructed image is high, and the mathematical formulation can be analytically derived starting from the Fourier transform of the object function. It is worth mentioning in this context that simple back projection of the measured data profiles (figure 5) does not produce a good reconstruction because each ray sum is applied not only to points of high linear attenuation

coefficients, but also to all points along the ray. This defect shows up most strikingly with discrete areas of high density, or 'hot spots', producing a star artifact.

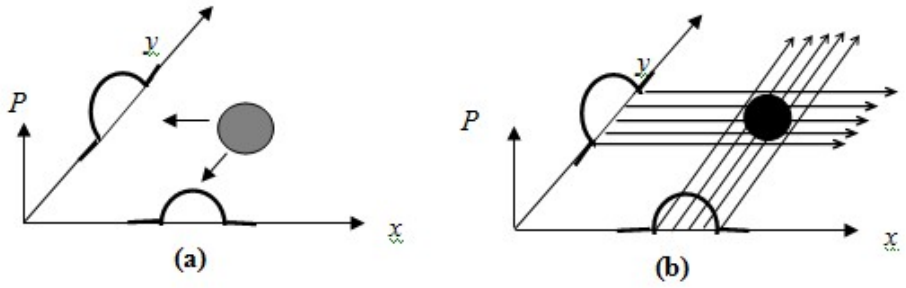

FIG. 5. Forward projection(a) and simple back-projection (b)

A detailed treatise on the subject of filtering the direct measured projection data in spatial frequency domain or convolving in spatial domain and then back projecting the modified projection data set in image grid can be seen in [4]. Discrete implementation of convolving the projection data and back projection can be achieved using the formula given by [6]. In the derivation, the filter function used is called a ramp. This ramp filter usually is referred to [7] as the Ram-Lak filter, after Ramachandran and Lakshminarayanan [8].

2.4.DIVERGENT-BEAM TRANSMISSION TOMOGRAPHY

In the preceding section, it was mentioned that a single source-detector configuration can be used for the generation of required projection data for the tomographic image reconstruction in a simple way. However, the very fine detector pitch, object's maximum span across the circle of reconstruction and the fulfilment of efficient sampling conditions, considerably prolong the total scanning time. In addition, the limited exposure rate of radio-isotopic sources also puts a limit on the nuclear data acquisition times. However, most of the total scanning time is taken up by the translation motion only. The rotate-translate mechanism used in single detector configuration can be modified to rotate-only mechanism with the use of multiple detectors and using a thin slice of the conical diverging radiation beam (figure 6), also called a fan-beam, emanating from the point-like source. However, a typical projection acquired with such a configuration of source and multiple detectors does not resemble a parallel-beam projection profile acquired in the same geometry.

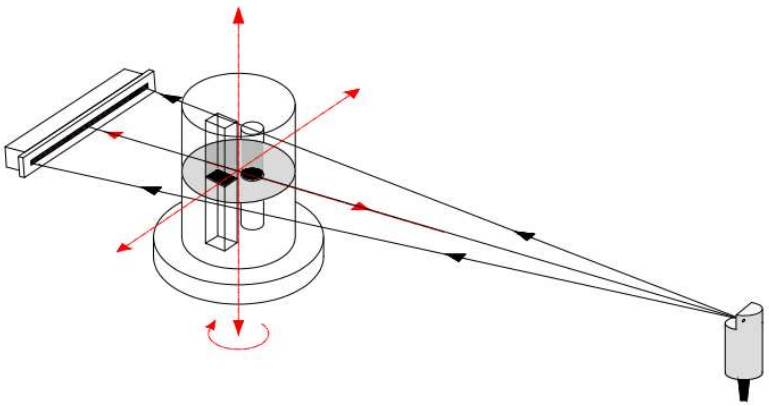

FIG. 6. Divergent bean (Fan-beam) in planar ICT

It may also be possible to arrange the multiple detectors along a line and which are equi-spaced, or, along a curve whose focal point coincides with the centre of the radiation source. In the latter case, each detector element subtends an equal angle at the focal point. This configuration is called to have an equi-angular detector array while the former one is called equi-spaced linear detector array. Thus, the term 'Linear Detector Array' or LDA used throughout the text here actually stands for an equally spaced linear detector array. One advantage of using a simple linear detector array is that the geometry can be flexible in sharp contrast to the equi-spaced detector array where the source to detector distance is fixed as per the curvature.

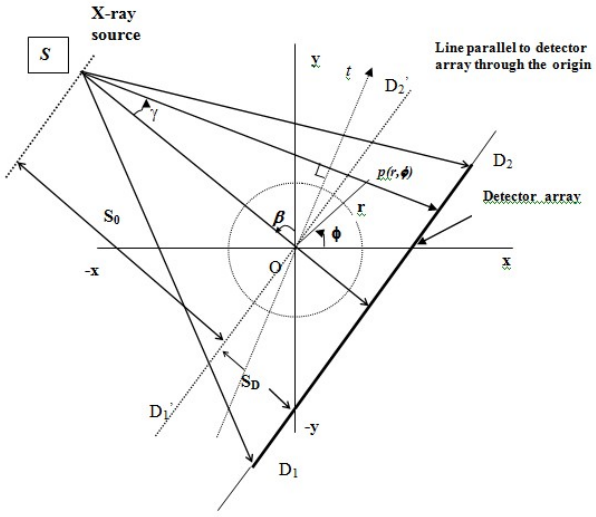

FIG. 7. A divergent projection scheme

In a tomographic scanning geometry specifically meant for imaging industrial specimen, the detector array and the radiation source (e.g. X ray tube assembly) are generally fixed and the object is subjected to a rotary motion in case of rotate-only third generation scanning mechanism. However, in case of a line detector, the rays are not sampled equi-angularly but equidistantly along the dashed line (D_1' D_2') as shown above in figure 7. D_1D_2 represents the actual LDA position where the projections are sampled. $D_1'D_2'$ is a virtual parallel line to D_1D_2. Other symbols shown in the figure are self-explanatory. Standard reconstruction algorithms for

such a hardware configuration can be adapted for generating the tomographic cross-sections through a given specimen. It should however be noted that there may be found many variations of the standard reconstruction algorithms e.g., short scan methods whereby angular scanning may be restricted to less than a full rotation to speed up the scanning.

2.5.SCANNING REQUIREMENTS

An image-based testing system cannot be better than the pictures produced by it. However, it is generally difficult to define the quality of a picture in an objective and unique way because visual perception is a very subjective procedure. There are four parameters affecting the quality of a tomogram i.e., spatial resolution, density resolution, noise and artifacts. The first three of them are not independent from each other. It means that only one of them can be optimized [9]. Assuming there are no sources for artifacts in the reconstructed image, parameters like the maximum object thickness, number of angular views for a given number of samples per projection in a given hardware configuration can be optimized. The distortions that arise on account of insufficiency of data are usually called aliasing distortions. Aliasing distortions may also be caused by using an under-sampled grid for displaying the reconstructed data [4].

2.5.1. Object thickness in the tomographic plane

For a given energy of the penetrating radiation used to scan a uniform object's cross-section of constant linear attenuation coefficient, the integrated attenuation along a path length depends on the material thickness. Alternatively, for a given path length, the total attenuation will depend upon the effective linear attenuation coefficients. If D is the diameter of the test object of constant linear attenuation coefficient μ, it is generally the product $\mu.D$, a dimensionless quantity, which can be optimized for the minimization of the relative accuracy ($\Delta\mu/\mu$) of the reconstructed image parameter. Gilboy [10] has arrived at an important equation relating the relative accuracy of the reconstructed attenuation coefficients to a 'sensitivity factor' expressed in terms of $\mu.D$. Retaining the original terminology, the equation is given as

$$\frac{\Delta\mu}{\mu} = 4\pi k N^2 \left\{ \frac{D}{tTA'} \frac{\sinh(\mu.D)}{(\mu.D)^3} \right\}^{1/2} \qquad (9)$$

In this equation, k is a constant which depends on the type of filter used; N is the length (in pixels) of the square image grid; t is the spacing between neighbouring rays in a projection; T is the total run-time and A' is given by $A'=A.q$; q being the detector's full peak intrinsic efficiency and A is the photon output per unit time of the isotropic point source. If all the geometrical factors, the total run-time and the source intensity are fixed, the accuracy depends upon the sensitivity factor $\left(\sinh(\mu.D)/(\mu.D)^3\right)^{1/2}$. A graphical plot of the sensitivity factor versus the number of mean free paths shows a broad minimum at $\mu.D=3$ as the photon energy is varied. However, the minimum is very shallow, and the relative error remains below twice the optimum value for $\mu.D$ values ranging between 1 to 6. It emphasizes that the choice is not very critical both in terms of the energy of the radiation used as well as overall maximum thickness of the test object at a given energy in this range.

2.5.2. Projection sampling and angular views

Let us take the case of a tomography system operating in a parallel beam geometry. In general, it will have a point radiation source and a detector with a collimator, which defines the spatial resolution in the image. The signal recorded by the detector will be integrated ray-sum over the full detector width. Thus, the detector collimator acts like a low-pass filter and information on sharp edges inside the object will depend much upon the sampling interval. An important question then arises as to how finely the sampling must be carried out for a given detector width. Nyquist criteria suggest that a signal must be sampled at least twice during each cycle of the highest frequency of the signal. If we assume T_d to be the detector width along the line projections are sampled, then the signal will essentially contain a maximum spatial frequency of $1/T_d$ (cycles per unit length). The sampling frequency will then be $2/T_d$. Consequently, the minimum sampling interval T_s can then be $T_d/2$. In simple terms, it implies that at least two samples must be taken per detector width. In the parallel beam geometry, this can be accomplished easily.

Once the number of samples in a projection is fixed, it is required to find out the number of angular views, which may be necessary to recover the approximate distribution of attenuation values in the defined image grid. A detailed theoretical analysis [4] based on the assumption that in the frequency domain, the worst-case azimuthal resolution should be approximately the same as the radial resolution yields the equation relating the number of samples per projection (N_S) and the number of equi-angular views (N_P) as

$$\frac{N_P}{N_S} \approx \frac{\pi}{2} \tag{10}$$

It has also been stated that for a well balanced $N \times N$ reconstructed image, the number of rays in each projection should be roughly N and the total number of projections should also be roughly N. However, the number of non-zero density values in $f(x,y)$ that must be determined is approximately $\pi N_S/4$. Brooks and his colleague [6] have therefore suggested that only

$$N_P = \frac{\pi N_S}{4} \tag{11}$$

angular views or projections are required.

A number of authors have examined the optimum relationship between N_S and N_P, but a choice in the range

$$\pi N_S/2 \geq N_P \geq \pi N_S/4 \tag{12}$$

is not too critical [10].

2.6.NOISE AND ERROR IN RECONSTRUCTED DATA

NDT imaging methods based on the computational tomography using γ-rays and X-rays are bound to have certain noise characteristics in the final data grid. This arises due to the fact that the penetrating radiation used has itself some statistical properties. Besides this, the computational procedure introduces some errors. The overall noise pattern is enhanced because

of other factors like errors in measuring devices etc. It is not possible to design and develop a tomography imaging system without noise. Even if electronic noise and scatter noise are minimized, quantum statistics dictate that there will be a variation in the number of gamma or X ray quanta detected. The photon noise of the radiation is known to obey Poisson statistics. Simply it means that the variance of the signal is equal to its mean. If an average of n photons is detected in a given sampling period, the number actually recorded will be in the range $n \pm \sqrt{n}$ approximately to 70% of the time.

The reconstruction process complicates the noise behaviour of the final image. As discussed above in the preceding sections, the projection data is convolved with a filter prior to back projection in the image grid. Naturally the convolution filters will alter the noise pattern in the reconstructed image. It has been shown that noise at the centre of a reconstructed cylinder of radius R_0 exposed by the incident penetrating radiation of effective energy E_{eff} for the Ramachandran (σ_R) convolution filter is given by the following equations:

$$\sigma_R \approx \frac{0.91}{s\sqrt{N_P}}\sigma_d \tag{13}$$

In this equation, s is the spatial sampling increment, N_P is the number of angular views and σ_d is the standard deviation of the noise on the samples in the profile data [11].

As it is evident, the projection data is the natural logarithm of the ratio of the intensity of the un-attenuated radiation n_0 and the detected signal n_t. The computation of the noise figure on the profile data is therefore complicated. However, in an approximation that the photon noise dominates, the maximum possible data noise σ_d is given by the following expression:

$$\sigma_d \approx \left[\frac{1}{n_0 \exp\{-2\mu_0(E_{eff})R_0\}} + \frac{1}{n_0}\right]^{1/2} \tag{14}$$

in this equation, $\mu_0(E_{eff})$ is the linear attenuation coefficient of the cylinder.

The two equations (2.13) and (2.14) suggest that the noise decreases with increasing photon counts and angular views and increases with increasing the radius and/or the linear attenuation coefficient value of the test object. Another expression for reconstruction noise has appeared [12].

Experimentally, the usual process of determining the standard deviation σ, for a homogeneous area of reconstructed image containing m pixels, each with some value μ_i, is by using the following two expressions:

$$\overline{\mu} = \frac{1}{m}\sum_{i=1}^{m}\mu_i \tag{15}$$

$$\sigma = \left[\frac{\sum_{i=1}^{m} (\mu_i - \bar{\mu})^2}{m-1} \right]^{1/2} \tag{16}$$

Where $\bar{\mu}$ is the mean value of m pixels.

The noise in a reconstructed image does have a positional dependence, especially near the edges of an object.

There has been some work by Munshi and others [13] devoted to studying the difference between the reconstructed image and the true values of the linear attenuation coefficients in the scanned object plane. If the projection data are band-limited, then using a Ram-Laks filter with the appropriate cut-off spatial frequency, it is possible to obtain a reconstructed image where the error is zero. However, in practice, the cross-section of the object being scanned has finite support, the projection data are not band-limited and the error between actual and reconstructed linear attenuation coefficients depends on the convolution filter. In this instance, use of the Ram-Laks filter with the cutoff spatial frequency set to the sampling frequency produces images with the smallest errors [7]. This aspect of the image reconstruction theory may be utilized in the development of the computer codes which may also be used in the studying the imaging characteristics.

2.7.CONTRAST SENSITIVITY AND SPATIAL RESOLUTION

Contrast of an industrial CT image is the property by which a feature in the image can be distinguished from its background or surroundings. The theory says that it is the voxel-averaged linear attenuation coefficient in the given plane of the object at the effective energy, which is reconstructed. Linear attenuation coefficients are functions of the incident energy of the radiation used. The sketch in figure 8 shows the functional dependence of the linear attenuation coefficients on energy for two different materials. The degree of contrast $\Delta\mu$ between the two materials will eventually depend on the energy at which the scan has been taken. In a general sense, it appears that for a given object configuration, choosing a low energy radiation will give a higher contrast. However, the choice of the energy will depend on other factors like full scale reading of the data acquisition system and the dynamic range.

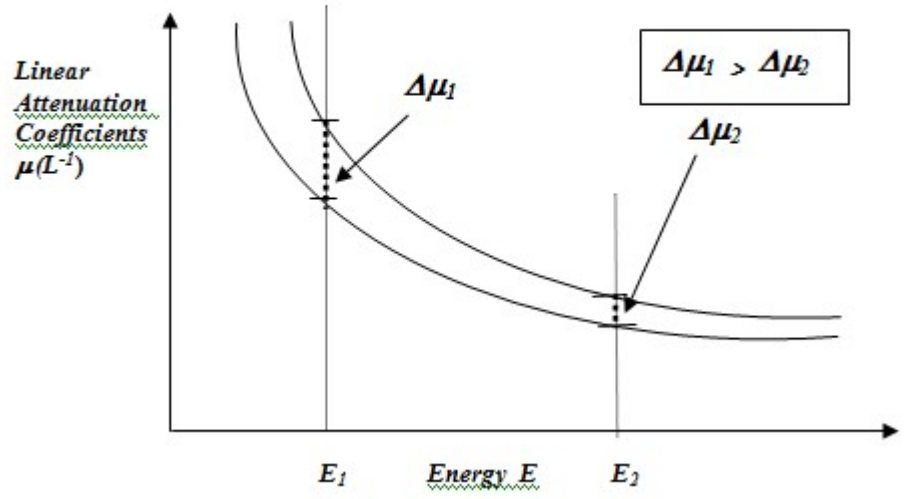

FIG. 8. Linear attenuation coefficient vs. energy for two different materials

In a test specimen, if μ_f and μ_b be the reconstructed linear attenuation values of the feature and the background then percentage contrast is defined as

$$Relative\ Contrast(\%) = \frac{|\mu_f - \mu_b|}{\mu_b} x100\% \tag{17}$$

This expression will not hold good if $\mu_b = 0$, i.e., when the background material is air. Also, it is assumed that the feature extends throughout the slice thickness. If the slice thickness is h_{slice} and the feature is having a thickness $h_{feature}$ then the contrast will be reduced by a factor $h_{feature}/h_{slice.}$ Also, the feature should occupy a significant number of image grid points otherwise due to the noise and degradation in sharpness of the edges in the reconstruction process, the feature may not be well defined.

Spatial resolution is a measure of the ability of an imaging system to identify and distinguish small details. In an X ray based ICT system using a linear detector array, the effective beam width of the penetrating radiation affects the spatial resolution of the imaging system. Factors that affect resolution include, source size, degree of geometric magnification, detector aperture and the reconstruction algorithm. An approximation to the effective beam width also known as the effective aperture size is given by:

$$a_{eff} \approx \frac{\sqrt{d^2 + [a(M-1))]^2}}{M} \tag{18}$$

where a is the width of the X ray focal spot and d is the width of detector aperture. The variable M is the magnification factor given by (figure 7):

$$M = \frac{S_O + S_D}{S_O} \tag{19}$$

where S_O is the source-object distance and S_D is the object-detector distance.

It is obvious that the finite number and width of the beam causes the blurring of a feature, which can alter both the shape of the feature and the resolvability of multiple features. The blurring also affects the perceived contrast. The blurring function called the point-spread function (PSF) is the response of the system to an ideal point object. The measurement of PSF can be made on a CT system by imaging a fine wire oriented perpendicular to the slice plane. If the pixel spacing is very close to the resolution of the system, the extent of the PSF may be only a few pixels and it will not be well characterized. The modulation transfer function (MTF) is a plot of the ability of the imaging system to transfer a sinusoidal signal versus the frequency of that signal. Fabricating such a test object is quite impractical and therefore alternative techniques are employed to experimentally obtain MTF. Spread function methods provide measurement of MTF from the modulus of the Fourier Transform of the line spread function which itself can be derived by differentiation of an edge trace. The MTF is defined as [14]:

$$MTF(\nu) = \frac{\left| \int_{-\infty}^{\infty} L(x) e^{ikx} dx \right|}{\left| \int_{-\infty}^{\infty} L(x) dx \right|} \tag{20}$$

where $k=2\pi\nu$, ν is the spatial frequency and L(x) is the line-spread function (LSF).

The LSF is roughly well-shaped function that drops to zero at, or before $\pm \propto$.

Normally, L(x) will be negligibly small and assumed to be zero at some value $\pm r_0$, so ex. (2.20) can be written as:

$$MTF(\nu) = \frac{\left| \int_{-r_0}^{r_0} L(x) e^{ikx} dx \right|}{\left| \int_{-r_0}^{r_0} L(x) dx \right|} \tag{21}$$

Experimentally, ERF denoted as *E(x)* can be measured by imaging an object with sharp density boundary and the first order differentiation will give the line spread function i.e.,

$$L(x) = \frac{dE(x)}{dx} \tag{22}$$

such that

$$MTF(\nu) = \frac{\left| \int_{-r_0}^{r_0} \frac{dE(x)}{dx} e^{ikx} dx \right|}{\left| \int_{-r_0}^{r_0} \frac{dE(x)}{dx} dx \right|} \tag{23}$$

It can be shown that the one-dimensional profile of a circularly symmetric PSF is roughly equivalent to a profile taken perpendicular to the two-dimensional response of the system to a line i.e. LSF. Some other methods for the determination of MTF can be found in published literature.

2.8.CONCLUSION

From the foregoing theoretical discussion on the tomographic image reconstruction and the related expressions based on the literature survey, it is clear that experimental tomographic imaging systems can be developed and applied to non-destructive testing and evaluation of industrial specimens. The concepts and mathematical formulations described above may be used to develop computer codes which, along with some suitable radiation sources, detectors

and scanning devices, would be useful to study some of the aspects of industrial tomographic imaging.

3. MONOCHROMATIC GAMMA RAY BASED PARALLEL BEAM ICT

The tomographic imaging method for non-destructive testing (NDT) is basically a process of collection of data through an object and then subsequent reconstruction of a two-dimensional image from the set of one-dimensional radiation measurements corresponding to a cross-section through the object. In NDT, this technique is employed to obtain quantitative mapping of the distribution of approximate linear attenuation coefficients inside an object for the given energy of the penetrating radiation. It requires special computing procedures to calculate the parameters of interest, (normally beam attenuation coefficients), which is in sharp contrast to the conventional radiographic procedure where one maps in image form, the total integrated absorption of penetrating radiation through an object.

3.1. INTRODUCTION

Monochromatic gamma ray based industrial computed tomography for non-destructive testing and examination are basically planar ICT imaging arrangement which are different from what is called process tomography systems mainly used in chemical and process trouble-shooting problems. Process tomography is not meant to provide high resolution cross-sectional images, which appears similar to gamma or X ray radiographic images. A tomographic image meant for NDT purposes of industrial specimen is expected to provide photographic-quality data having acceptable spatial details and contrast specified by the imaging parameters.

There are certain distinct design modifications in comparison to the medical transmission CT scanners, where object parameters are fixed thereby defining the system operating domain. In case of ICT, one has to take into account varied range of material specifications as well as geometry to arrive at a particular configuration which includes beam energy and energy spread in the penetrating radiation. An ICT scanner in single-detector configuration utilizing monochromatic gamma rays from a sealed radioisotope source is comparatively easy to assemble for teaching and demonstration purposes in the laboratory. Computed tomographic imaging system based on monochromatic penetrating radiation has some unique advantages over a polychromatic beam like X rays. Use of a monochromatic radiation source in such imaging applications does not cause beam hardening effect and a moderate source intensity makes it possible to design the data acquisition system to operate in pulse mode. This facilitates to easily analyze the system performance. Though any other source can also be used, multiple energies in the probing radiation may produce a map of reconstructed linear attenuation coefficients which may be difficult to analyze. Certain radio-isotopic sources offer a good combination of energy, half-life and practical availability suitable for industrial CT applications. ^{137}Cs is a radiation source having a half-life of around 30 years and the energy of the gamma rays is 662 keV. The relatively long half-life of this radioisotope is quite suitable for prolonged use in industrial tomographic imaging without frequent decay correction and the single energy of 662 keV offers a good penetrating capability in thick objects also.

3.2.OBJECTIVE

The objective is to understand the basic building blocks of a simple gamma ray based ICT scanning mechanism. It should however be noted that the ICT configuration for NDT applications makes use of large number of very precise radiation measurements through the specimen at the given tomographic plane. Therefore, some degree of automation would be inherent as it would be very difficult to acquire such data for tomographic reconstruction. The following sections will elucidate the major sub-systems and their functions.

3.3.BASIC BUILDING BLOCK

Most conventional ICT scanners fall into one of four generations. The first and second-generation systems are suited for many low speed industrial research applications. The strength of first generation systems is their low cost because of simple design and extremely simple geometry and data collection scheme. These systems use only a single detector and there would possibly be almost no variation or small mismatch within various regions of the entire data set. Besides these, operation of a first generation system can be made fully computer controlled for scanning mechanism and data acquisition system in a rather simple and straight forward manner.

This section will focus on the details of a typical experimental system. A typical first generation system as shown in figure 9 comprises of mainly three major sub-systems : (i) beam generator containing optimal strength (activity) of either ^{137}Cs or any other radioisotope equipped with a beam ON/OFF mechanical assembly and a source collimator; (ii) a single NaI(Tl) – PMT integral assembly in a thick shielding enclosure with a removable detector collimator head and (iii) a preferably three-axis stepper motor controlled mechanical manipulator. The size of the scintillator crystal is also important as the intrinsic efficiency and energy resolution will vary accordingly. Though the front collimator of the detector assembly may have a very fine slit width, a crystal size of 1” x 1” through 3” x 3” may provide efficient counting statistics for better signal to noise ratio.

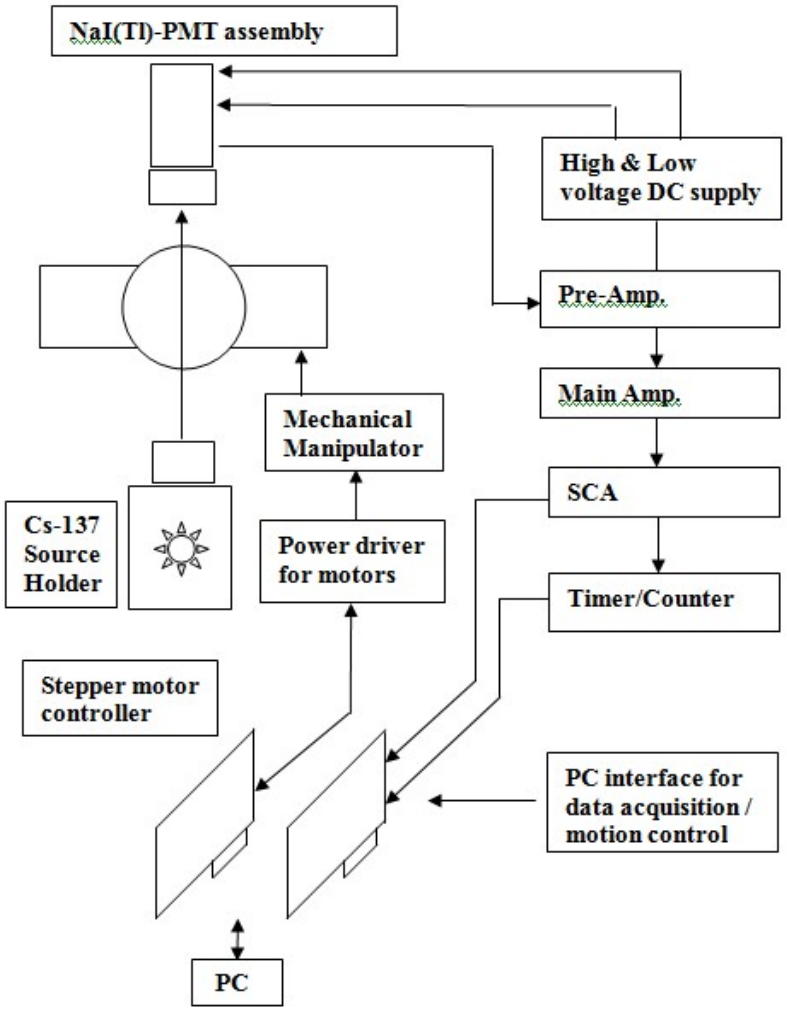

FIG. 9. Schematic diagram of a typical single-detector ICT scanning mechanism

3.4.GAMMA SOURCE AND DETECTOR ASSEMBLY

3.4.1. Radiation exposure configuration

The emission of gamma rays from a radioactive source is a nuclear phenomenon and as such, exposure devices using such radiation sources are primarily designed for containing the continuous radiation emission. This is required to meet the radiological safety aspects also. Generally, gamma sources have a small source size (0.5 mm -10 mm) and such sources may be considered as a point source. The beam generator used in the experimental system is basically a source container equipped with a mechanism, to allow or to stop a narrow beam of gamma rays to come out. A collimator designed to further reduce the emerging gamma rays to a pencil beam (~5mm dia.) is placed adjacent to the source container. Figure 10 shows a section of a typical arrangement as viewed from top of the source-detector assembly. A 3" x 3" single NaI(Tl) scintillator – photo multiplier tube (PMT) assembly enclosed in a separate lead-shielded detector housing has been used for detecting the transmitted flux through the object. It can be seen that the incident radiation through the collimator falls on the detector crystal.

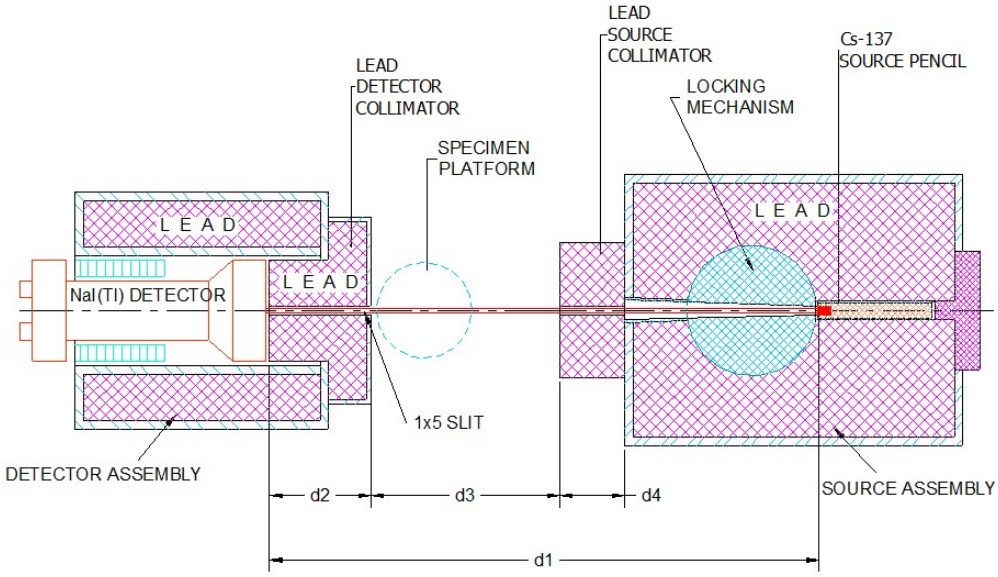

Typical dimensional values: d1~500mm, d2~50mm, d3=200mm, d4~100mm

FIG. 10. A cross-sectional plan view of source-detector assembly

3.4.2. Single detector configuration

A three-inch standard crystal size along the beam path may be selected so that around 90% of the incident gamma photons may be absorbed. A fixed detector collimator (typ. 1mm x 5mm) made of lead with steel lining may be used for having approx. 1 mm^2 pixel resolution in the ICT plane with a slice thickness of 5 mm. The detector enclosure has been designed to cut off scattered radiation from reaching the scintillator crystal while the front detector collimator serves the basic purpose of achieving an optimum tomographic resolution taking into account factors like total scanning time and achievable counting rate. It may be emphasized here that significant scattered radiation reaching the detector surface plays a detrimental role in the overall image quality.

The light emitted by a scintillator material as a result of interaction of gamma ray or X ray photons with the medium must be detected using some kind of light-sensitive detection device. Broadly, there are two options: (a) using a photo multiplier tube (PMT) and (b) semiconductor based photodiodes (PD).

In a PMT, light photons generated in the scintillator material are converted into *photoelectrons* by absorption in a thin photo cathode layer inside a (glass) vacuum tube. Mostly a photo cathode is semitransparent and usually consists of a thin layer of evaporated Cs, Sb and K atoms or a mixture of these. Each photoelectron is pulled by an electric field towards a dynode and subsequently amplified. Each scintillation pulse produces a charge pulse at the anode of the tube. A typical PMT tube may provide amplification of the order of 10^6. This is normal way to operate a PMT in pulse mode. PMTs can also be operated in current mode in which case, the anode current is measured for the integral radiation intensity absorbed in the scintillator material. In spectroscopic measurement systems, the scintillator-PMT assembly is operated in pulse mode. The pulse height is a measure of the energy of the incident gamma-ray photon. Figure 11 shows a schematic block diagram of a standard scintillator-PMT set-up. The processed pulse signal from the main amplifier can be fed to a multi-channel analyzer for spectroscopy applications or to single channel analyzer so that the gated TTL pulse train is further synchronized with a computer-controlled manipulator and digitally stored, as in a tomography set-up.

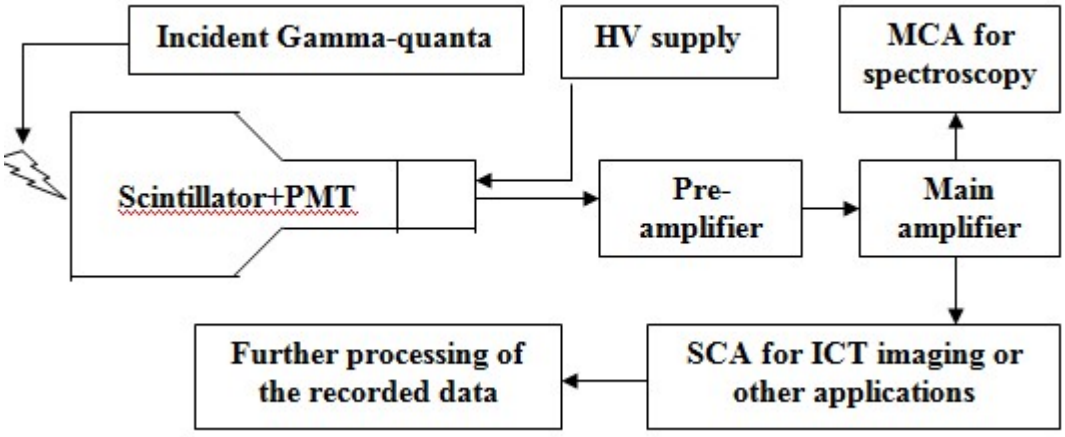

FIG. 11. A typical gamma-ray counting set-up using PMT

3.4.3. Gamma-ray beam characteristics

For intermediate size scintillator detectors like the ones suggested here, the spectrum for low to medium gamma ray energies (where pair production is not significant) consist of a Compton continuum and photo peak. Because of multiple events to the photo peak, the ratio of the area of the photo peak to that under the Compton continuum is significantly enhanced. Figure 12 is a multi-channel analyser plot of the detector response with a standard ^{137}Cs source when the detector-PMT unit was outside the lead-shielded enclosure. This response shows an energy resolution of ~13% (photo-peak area) which is normally expected from a NaI(Tl) scintillator of this size. The high voltage applied to the PMT was 600 Volts.

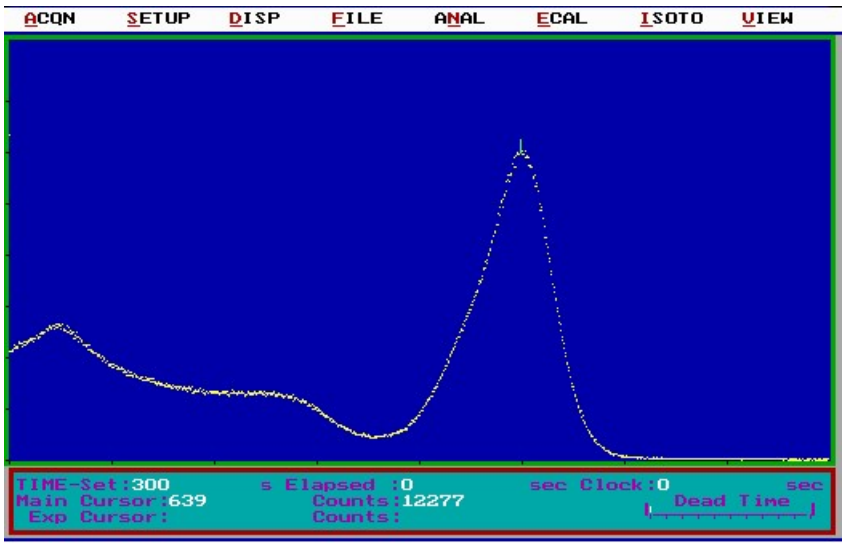

FIG.12. Multi-channel analyser plot of the detector response with a standard ^{137}Cs source (detector-PMT unit outside lead-shielded enclosure)

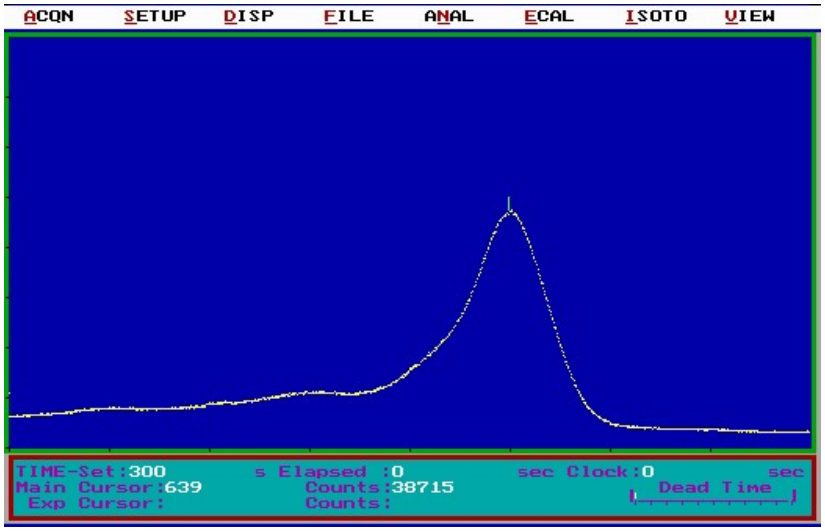

FIG. 13. Multi-channel analyser plot of the detector response with a standard ^{137}Cs source (detector-PMT unit inside lead-shielded enclosure with collimator)

The counting time needs to be adjusted so as to take care of the incident flux from the selected source. It is seen that the profile is modified with the photo-peak becoming broader and a less significant scatter region when the scintillator-PMT assembly is heavily shielded (figure 13). In any practical application, the effect of surrounding material can have a major influence on its response. This response of the detector in the given configuration is suitable for tomographic imaging for non-destructive applications. A proper threshold and window around the photo-peak through the SCA used in the data acquisition system would be desirable in such applications.

3.5.SUGGESTED STEPS-TO –FOLLOW

The first and foremost requirement in setting up a small gamma ray based ICT for NDT in the laboratory is to define the maximum object or test specimen dimensions, the special resolution expected in the tomographic plane, total scanning time and simplicity in object maneuvering.

It is also important to limit the maximum material thickness which may come in the beam path at any possible angular position during scanning time. While the specimen dimensions would define the circle of reconstruction (COR), the maximum material thickness would define the signal to noise ratio in the projection data recorded. When there is no material thickness in the beam path, the detector sees the direct beam. The counting time should be selected in such a way that the detector response remains in the linear range. The judicious selection of d1, d2, d3 and d4 (figure 10), slit width and height of the detector collimator, the source activity and the counting system parameters (e.g. gain) may help in arriving at a system configuration which generates error-free projection data for good reconstruction. Figure 14A and figure 14B pictorially shows source and detector assembly and their relative positions with respect to the object platform. The dimensions are not to scale.

If n_b, n_{tl} and n_0 are the average back-ground counts, minimum counts (when the beam path encounters maximum attenuation) and maximum counts (through the air and no object attenuation in the beam path) for a given counting time (t), it would be advisable to have $n_{tl} / n_b > 10$. n_0 / n_{tl} would depend upon the attenuating factor. If a maximum of two TVL equivalents object thickness is expected at any angular position at the energy of the penetrating radiation, it would necessitate a high activity source and a wide dynamic range counting system. For example, on an average, if n_b is assumed to be 30, n_{tl} would be 300 and n_0 would be 30000 for a counting time of t seconds. The attenuation through the air may be assumed negligible (figure 15). The diameter of the circle of reconstruction may be kept small as compared to the distance d1. This may help to assume the intensity of the beam just before entering the object as close to n_0.

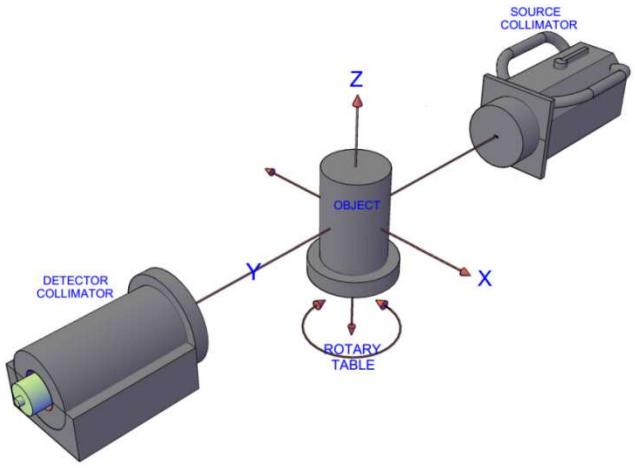

(14-A)

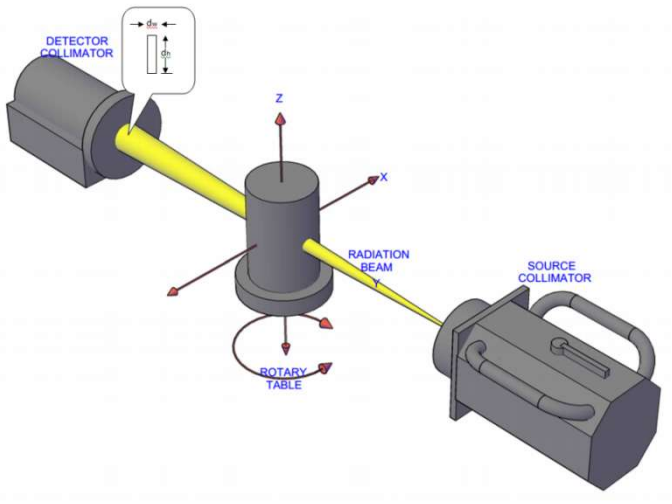

(14-B)

FIG. 14 (A) & (B) Pictorial representation of source and detector assembly and their relative positions with respect to test specimen (not to scale)

Once n_0 is defined, the source activity can be approximately calculated based on simple geometry assuming an isotropic sealed point source contained in the source assembly (figure 10). If d_w and d_h are the detector slit width in the scanning plane and along the vertical axis respectively and d_1 is the source to detector distance, it can be shown that

$$n_0 = \frac{3.7x10^{10}.A.(d_w.d_h)}{4\pi d_1^2}.\varepsilon_{\text{int}}.r \qquad (24)$$

where A is the radioactive source activity (Curies). ε_{int} is the intrinsic efficiency of the detector and r is the peak-to-total ratio in the spectra. n_0 is the total counts recorded by the counting system when single channel analyzer (SCA) is tuned to allow only the photo-peak area to be recorded as specified in section 3.4.3.

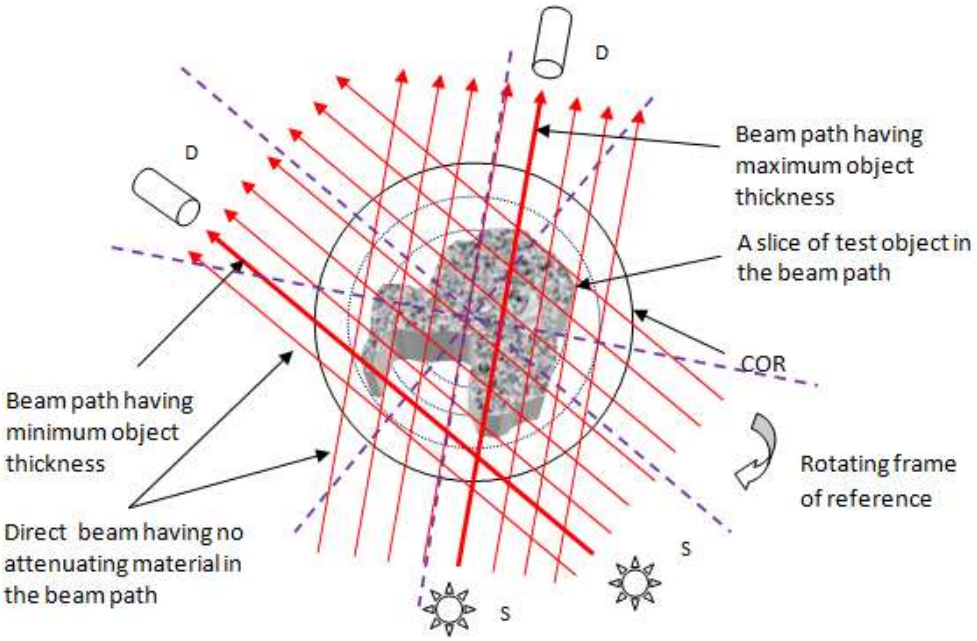

FIG. 15. A slice through the specimen in the beam path

The total counting time per slice scan would become (Ns.Np.t) seconds where Ns and Np are the number of samples per angular view and number of angular views over 180^0 for a parallel beam geometry scanning configuration. This is in addition to the total time taken by the mechanical movements in start-stop sequences spanning over the entire circle of reconstruction and all angular views.

The source detector assemblies defining the beam line and the mechanical movement axes must be aligned properly. There must not be any precession in the rotary table (axis z) and the relative angular positions as shown in figures 14 A-B, 16 and figures 17 A-C must be ascertained. These are important as any error in these mechanical alignments will give rise to sharp artifacts in the reconstructed images. The object table should be as close to the detector plane as possible to minimize scatter radiation. Figure 16 shows the top view of the scanning mechanism. As evident, the source-detector assemblies are fixed so is the radiation beam profile.

The specimen platform (COR) moves across the beam in a start-stop fashion to cover the entire region. When an entire projection is recorded, the table rotates by an angular increment and the sequence is repeated either uni-directionally or bi-directionally. Depending upon scanning sequence, the recorded counts may require resorting before projection values are calculated.

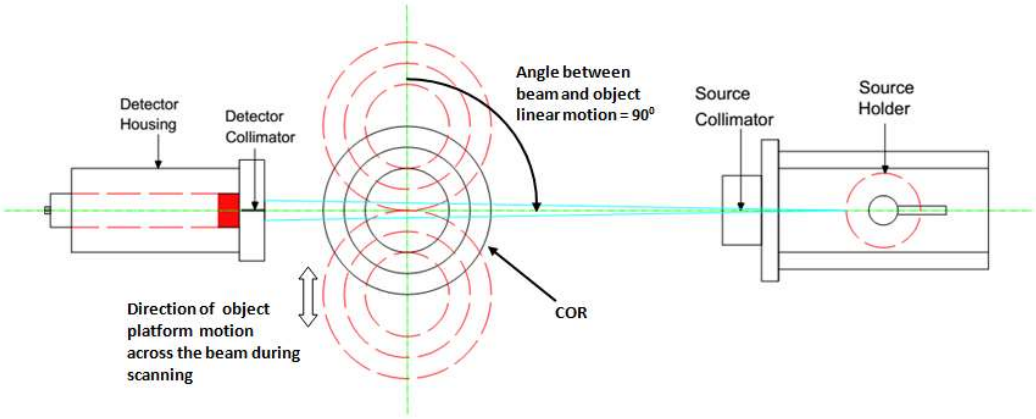

FIG. 16. Top view of the scanning arrangement

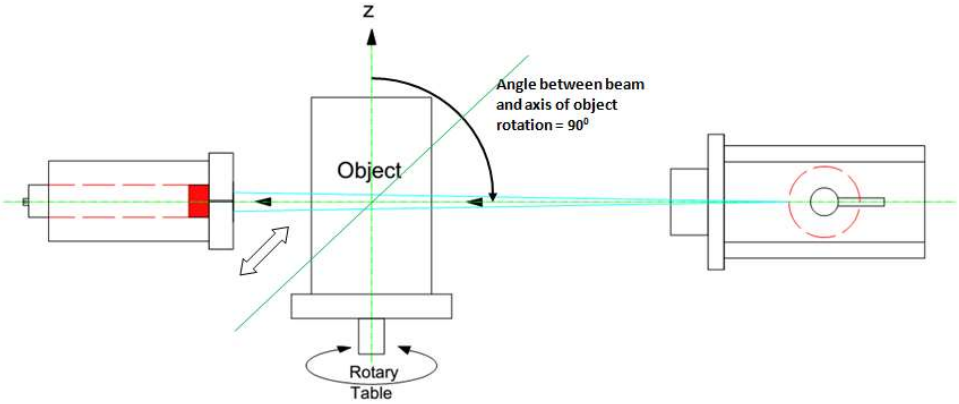

(17-A)

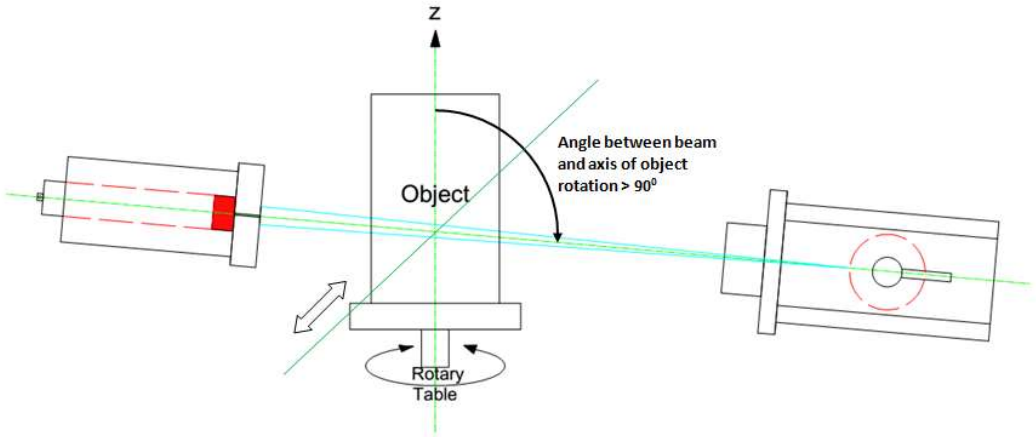

(17-B)

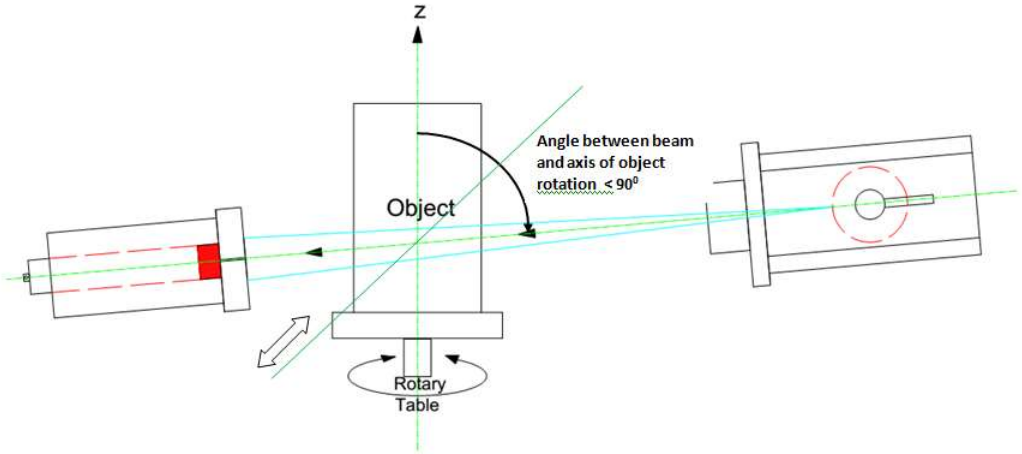

(17-C)

FIG. 17 (A-C). Orientation of the radiation beam with respect to the axis of rotation.

Correct position is shown in fig. 17A.

Among the numerous possible scanning sequences in case of first-generation ICT including techniques to measure n_0, a simple and novel idea would be to restrict objects well within the circle of reconstruction and acquire transmitted intensities (direct scan points) a little bit outside the object domain as shown in figure 18. This would allow computation of projection profiles independently for each angular view. This would also help in mitigating effects of small temporal variations in the counting system beyond the statistical factors. However, the number of direct scan points may preferably be limited to 5-10% of N_s so as to arrive at an average value of n_0 with better statistics for each projection angle. In extreme cases, the detector should be able to record at least one or two direct beam counts.

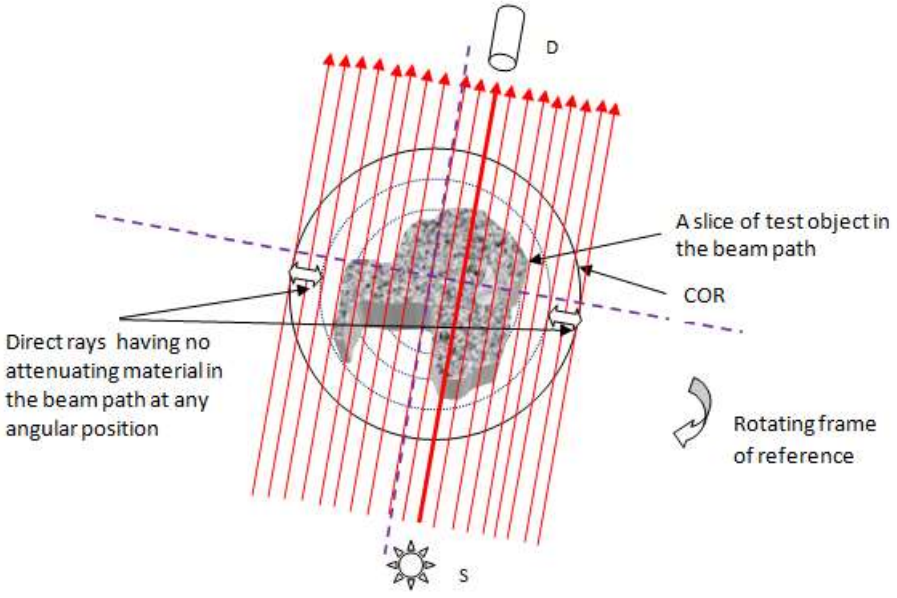

FIG. 18. Technique to record direct beam intensity while measuring the attenuated intensities through the test specimen

As evident, there is only one source-detector arrangement and thus we have a very fine beam of gamma rays which has to traverse across the entire object cross-section at the selected plane to generate one set of discrete projection data (N_s points). This has to be repeated N_p

times at equiangular positions over 180^0 to generate N_p sets of discrete projection data for discrete implementation of convolution and back projection.

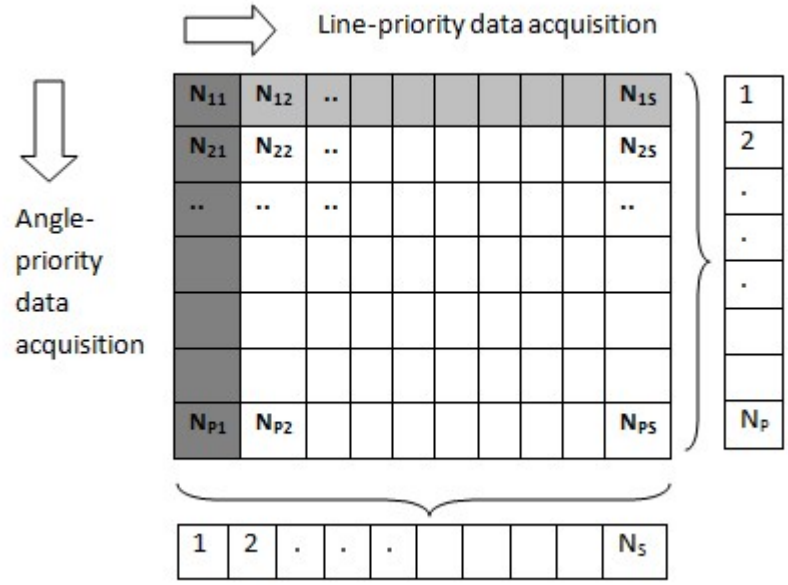

FIG. 19. Arrangement of recorded transmission data (counts) in a table

As shown in the figure 19, the recorded transmission data (counts) are stored in a tabular format. The table needs to be completed in order to calculate projections and later build a sinogram. It would not make a difference whether first the rows are filled from left to right or the columns are filled from top to bottom. In the first scenario, transmission data across the test specimen are acquired at the designated sampling points and at the end the specimen is given an angular rotation and the same linear sequence is performed to complete the next row. It is also possible to acquire transmission data corresponding to all designated angular views by rotating the specimen table at a given linear position. This will provide a column of the table with recorded data. In case of a very precise mechanical manipulator, this may result in considerable saving in scanning time due to mechanical movements. However, the scanning system will need programming accordingly.

3.6.SYSTEM CONTROL

Hardware system control is very specific to the type and configuration of the hardware used to perform data acquisition. There may be numerous hardware solutions which may be provided by different vendors once the purpose and type of data required are specified to them. Possibly the simplest and cost-effective would be a generalized nucleonic counting system coupled with a two or three axis open-loop stepper motor controlled mechanical manipulator which are then properly interfaced to a personal computer. A generalized motion-control and data acquisition software system may then be developed or customized serving the specified purpose. It may however be noted that in addition to the tabular data as per figure 19, the preprocessing and reconstruction program may also require the system parameters e.g., numerical values of d_w, d_h, COR, N_s and Np in addition to specimen/slice number and date and time of scanning for proper data archival. A format of data storage may be devised which should be uniformly followed for uniform processing of data.

3.7.TYPICAL SYSTEM RESPONSE

A typical first generation ICT imaging system described in this chapter and operating in the translate-rotate mode is shown in figure 20. The scanning sequence can be described in the

following way. The specimen platform is brought to the initial position at the start of the scan. The linear increment, number of samples per projection, number of total angular projections and the counting time are programmed in the control program. For each relative source-detector position defined by the instantaneous linear and angular coordinate values, total count is recorded for a given counting period and the process is repeated till the end of the scanning sequence. Thereafter, the data is pre-processed for calculation of projection data prior to image reconstruction. The response of the imaging system is basically to look into its behavior in terms of reconstruction linearity, spatial resolution, contrast sensitivity and statistical noise properties under the given operating conditions. The detector collimator has a slit width of 1.0 mm in the horizontal tomographic plane and 5.0 mm along the normal to this plane (Table 1). The former one is primarily responsible for the spatial resolution in the tomographic plane. Therefore, a spatial resolution of 1 mm is expected in the reconstructed image. This has been tested by scanning a resolution test block. As shown in the figure 21A, five holes of different dia. were drilled in a solid square steel block (50 mm x 50 mm). The tomographic image obtained after scanning this test block on the experimental system shows all the five holes. However, the contrast is reduced as the hole size approaches the detector aperture size. The image shown here is not to scale.

FIG. 20 (A-C): (A) Photograph of an experimental ^{137}Cs-based computed tomography System showing 1. radiation source assembly; 2. detector and 3. object manipulator, (B) detector housing and collimator and (C) a custom-made gamma counting system

TABLE 1: Scanning parameters of a typical ^{137}Cs-based computed tomography System shown in fig. 20.

Radiation source	Caesium 137

Energy	662 keV
Counting time per sampling point	0.4 to 1.0 s
Resolution of the PC based counter	16 bit binary mode
Circle of reconstruction	100 mm dia (typical)
Scanning step size	0.5 mm (typical)
Number of samples per projection	201 (typical)
Number of equi-spaced angular positions	100
Detector aperture	1.0 x 5.0 mm
Overall scanning time per slice	4-7 depending upon counting time

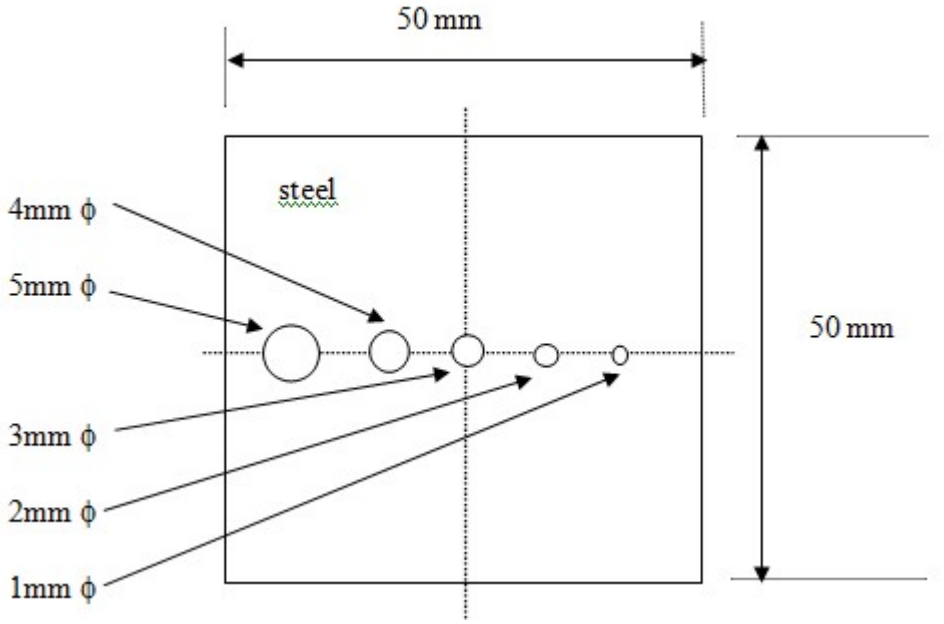

FIG. 21 A. A schematic cross-section of the resolution test block

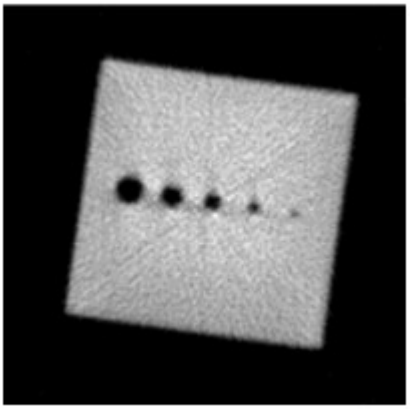

FIG. 21 B. A typical tomographic cross-section of the resolution test block

The contrast with which the designated defect of the limiting spatial resolution is visualized (figure 21 B) also depends upon the flux intensity and the total scanning time. In addition, the convolution filter also plays an important role in the overall performance. It has been established that the convolving function (or equivalently the filter function) controls the spatial resolution and noise properties of the reconstructed image [5]. By reducing the aperture size on the detector's collimator and the pixel width, one can increase the spatial resolution. All imaging systems, CT included, are limited in their ability to reproduce test object composition. That is, two regions of identical material will be imaged, not as smooth areas of equal reconstructed value, but as grainy areas of statistically variable values. Hence, upon repeated examination, the mean value of the two regions will vary randomly in relative magnitude. *Contrast discrimination* is a measure of this variability and obeys much the same rules as any other radiological imaging modality. The contrast resolution is the ability to reveal small differences in the linear attenuation coefficients in the object. It depends on the ability to distinguish signal from noise in the image and may be improved by increasing the counting statistics. Thus, both spatial and contrast resolution necessitate an extension of the data collection time [15].

This means, there is always a compromise between tomographic image quality (achievable contrast resolution) and data acquisition time. The next important one is system linearity. In simple terms, it means that if the linear attenuation value of the test object is increased, the average reconstructed value should also change by the same proportion. This is quite important as this behavior decides how an unknown object cross-section will be faithfully reproduced in terms of displayed grey shades. The graph as shown in figure 22 clearly depicts the remarkable agreement between the average reconstructed linear attenuation coefficients and the respective tabulated data in case of three materials. The data was generated on the translate-rotate monochromatic gamma computed tomographic system at 662 keV. It should however be noted that the reconstructed data is algorithm dependent. In a single source-detector system like the one described here; sources of major systematic artifact are not many except the one due to displacement error in the translation system. This will occur when the mechanical center of rotation is not located at the origin of the coordinate system as defined by the reconstruction algorithm's equation. The result is a characteristic streak pattern, dubbed a "tuning fork" [16]. The effect is prominent when the displacement is in a direction perpendicular to the 0^0 or 180^0 beam position. The simple way of reducing its effect to an unperceivable limit in the image is by carefully aligning the mechanical assembly to the scanning geometry. The reader is referred to see the paper [17] for some more results achievable on such system.

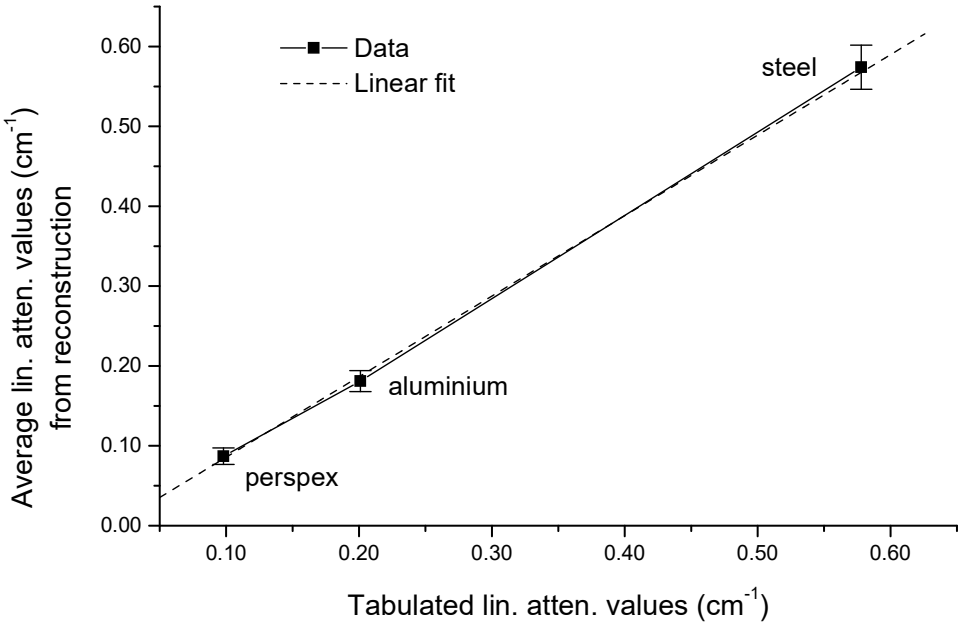

FIG. 22. A plot of average reconstructed attenuation values versus standard tabulated data in case of a ^{137}Cs-based first generation ICT system (the reconstructed data is algorithm dependent)

3.8.CONCLUSION

The chapter provided a very brief but concise treatment of the subject matter with respect to first generation ICT scanning systems for non-destructive applications. Some of the important steps which should be followed in configuring a typical system have been discussed. Important practical formulas based on literature survey were discussed in the preceding chapter for quantitative analysis of reconstructed data with the applicable limitations on the usability of such analysis. These can very well be applied especially in case of translate-rotate type ICT system using monochromatic gamma ray sources as the penetrating radiation.

4. EXPERIMENTAL X RAYBASED ICT USING A LINEAR DETECTOR ARRAY

4.1.INTRODUCTION

One of the limitations of the single detector configuration is the long scanning times. The scanning time is the total time taken by the mechanical movements as well as electronic data acquisition. As there is only one pencil beam, which is used for the complete scanning sequence, the scanning time becomes overtly long even for a fairly strong source activity. To reduce the overall scanning time and have faster throughput, one way is to use a fan-like beam of X rays or gamma rays and using an array of detectors placed along a line or a curve. The fan beam is achieved by using a proper collimator and the overall configuration follows certain scanning geometry. A typical scanning geometry may involve around 500 individual detector points. The system can still operate in start-stop mode without involving any translation motion. In this, the so-called third generation scanning mechanism, problems may arise due to non-uniform response of the detector pixels and it might manifest in different artifacts in the reconstructed tomographic images [18, 19, 20]. The problems are compounded in a modified scanning mechanism, where the object rotates continuously, and transmission data is acquired on the fly. The *standard* fan-beam convolution algorithm requires that projection data is available over a complete 360^0 angular view. The investigations suggest that in a situation where the last acquired projection does not correspond to the 360^0 angular positions, artifact would be introduced in the tomographic images, which have a unique characteristic. This chapter will however not delve into the genesis of all related artifacts.

4.2.BASIC BUILDING BLOCKS

An LDA based ICT operating in fan-beam configuration will basically have three main sub-systems on hardware side. These are (i) a suitable X ray generating equipment, (ii) a compatible linear array detector assembly and (iii) a programmable electro-mechanical manipulator device in addition to the control and data acquisition system preferably built around a personal computer. As stated earlier also, numerous configurations exist as regards type and variety of these sub-systems. A system integrator will be the most suitable person who can arrive at the optimum configuration of a proposed ICT system out of available hardware and software components available at his disposal. The selection will also be guided by the suggested specifications of the ICT by the user and the cost factors. In order to see the intricacies involved, a simple block diagram of a typical LDA based ICT developed for experimental studies in the laboratory is shown in figure 23. It normally contains a three-axis mechanical manipulator including the rotary mechanism, trigger components and the detector array, which is exposed to the radiation beam.

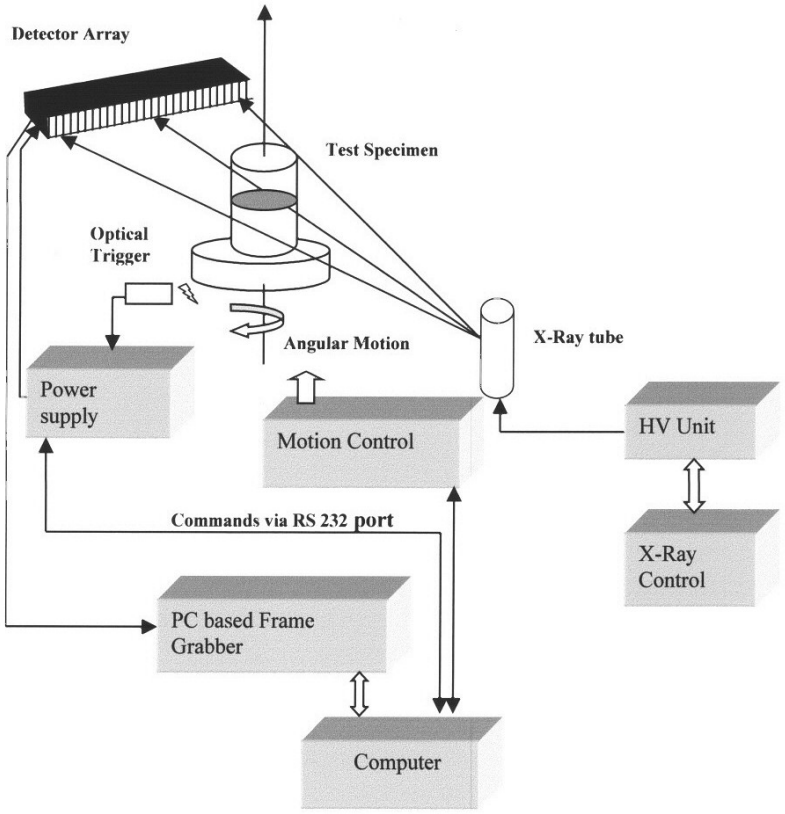

FIG. 23. Schematic diagram of a typical X ray based experimental tomography system using a low-cost LDA

4.3.X RAY SOURCE AND DETECTOR SUB-SYSTEM

General-purpose linear detector arrays (LDA) are routinely employed in baggage scanners and other online film-less radiography equipment. They are modular in design and for low energy X ray imaging applications, a typical LDA will have a linear array of photodiodes coupled with a thin layer of scintillator material in most cases GOS (Gd_2O_2S). The operations are rather simple – activated by an external signal, the line array acquires signal corresponding to incident X ray intensity on the constituent pixels. A single trigger will read multiple times the whole of the detector line to fill a data matrix in the computer memory. The acquisition time is very fast, and the output data is direct digital equivalent of the read intensities. The statistical fluctuations in the primary X ray beam intensity, X ray to light conversion, electronic noise and other system instabilities produce a number of false signals in the detector system. Even when the X ray beam is off, there is some noise signal generated in the imaging hardware. Besides these, there may be gain instabilities in individual pixels. All these add up to the noise in the final image.

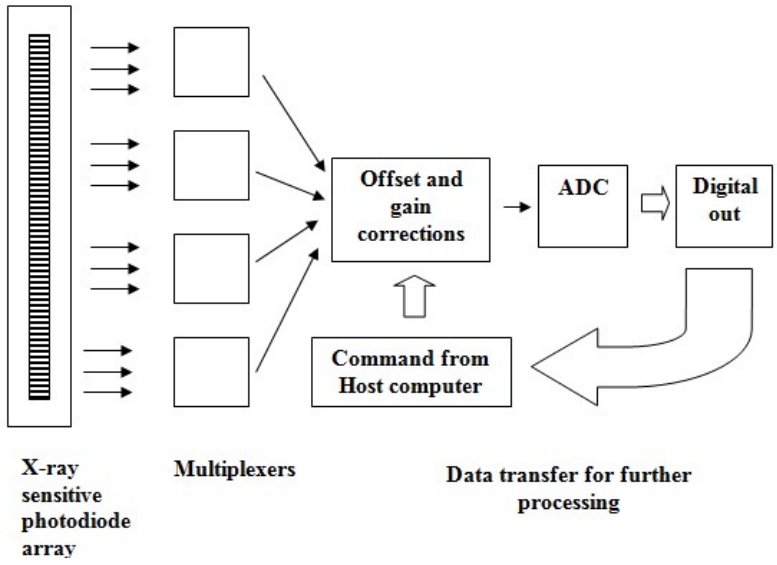

FIG. 24. Schematic functional diagram of a typical linear detector array system

The basic building block of an LDA is shown in figure 24. The X ray sensitive photodiode array consisting of 512-1024 pixel elements may be built of modules of lesser number of pixels. The scintillator converts the incident penetrating radiation energy into bursts of visible light, which are incident upon the photodiode sensitive area. The electrical signal is generally multiplexed and digitized using a 12- or 16-bit ADC. The digital signal will be corrected for offset and gain calibrations and then transferred to the host computer for further processing. Commercial-grade LDAs have been available for around twenty years or so and the technology has developed towards faster scanning speeds, better dynamic range and smaller pixel sizes. All such LDAs are designed mostly for current mode applications. The basic reason for current mode operation is the high flux (~10^7 photons/mA.s.mm^2 at 750mm from the source) from industrial X ray sources, which are preferred for short-time integration time, and large number of individual detectors resulting in faster throughput in simple transmission imaging applications. For simplified operations and integration, a constant-potential variable energy X ray generating equipment (40-220 kV) with a fine focus X ray tube may be acceptable. However, the choice of focal spot of the X ray system depends very much on the pixel size of the LDA in order to achieve an optimum spatial resolution in the ICT images. It should however be understood that the polychromatic nature of the X ray emission poses greater problems in image interpretation in addition to giving rise to specific artifacts in the reconstructed images. Table 2 lists some important parameters of a typical commercially available low-energy LDA.

TABLE 2. Typical Linear detector array specifications

Type of the detector system:	GOS Scintillator based linear diode array
Number of pixels:	512
Detector pixels used:	260
Pixel size:	0.8 mm (H) x 0.6 mm (W)
Detector pitch:	0.8 mm
Length of active area:	410 mm
ADC resolution:	12 bits
Control signal (PC to module):	via RS 232 interface
Data transfer (Module to PC):	via RS 422 interface
Onboard offset and gain calibration:	Yes
External Trigger:	Optical trigger sensor (reflecting type)
Make:	Xscan08 of Detection Technology Inc., Finland.

4.3.1. Calibration and optimization of LDA

An LDA is basically a one-dimensional scintillator screen coupled to a number of pixelized photodiodes at the back. An LDA based industrial computed tomography imaging system may be used for obtaining radiographic image of a given test specimen also provided the mechanical linear scanning capability exists. The spatial resolution and achievable contrast depend on the energy of the X-rays, characteristics of scintillator material and its thickness in the beam path as well as the overall electronics for data acquisition. In addition, the response of individual pixels to the incoming radiation also decides accuracy of the acquired projection profile. Most of the commercially available LDAs will have some hardware and software system supplied as part of the package to calibrate, optimize and evaluate detector response possibly as per applicable codes and standards. LDAs are always calibrated before usage to equalize the different characteristics of the detector elements. This avoids image distortions by fixed pattern noise due to differences in the detector elements and the electronics. Consequently, the image noise depends dominantly on the photon statistics. The reader may refer to standard guidelines ASTM E2736-10, ASTM E2698-10 and ASTM E2597/E2597M-14 for a detailed discussion on various aspects related to DDA as well as other published literature related to detector characterization.

A detailed discussion on linear detector calibration and optimization is out of scope of this technical report. However, contrast sensitivity and spatial resolution should be optimised before any such detector is used for radiographic or tomographic imaging applications. In addition to these, artefacts produced due to important hardware and software issues must be studied.

4.4.SYSTEM CONTROL AND SCANNING SEQUENCE

A three-axis PC based stepper motor controlled mechanical manipulator can be used for object manipulation and system alignment. The use of such system is a cost-effective option in place of closed loop servo drive based manipulators. To illustrate these requirements, a specific low-energy ICT which was developed in a laboratory is shown in figure 25 (A-B). The horizontal axis is parallel to the detector length and as such it is used for beam alignment. The vertical axis is used to select scanning planes and to move the object vertically in computed radiographic scanning mode. The rotary axis provides the specimen platform to hold the object and rotate. The source to detector distance (S_D) and source to centre of rotation distance (S_0) was set to be

1120 mm and 920 mm respectively. This configuration provided a geometric magnification of 1.22. In the experiment described here, only a portion of the full length of the linear array was used such that 260 detector elements symmetrically around the central ray fully covered the circle of reconstruction. This arrangement gave a fan beam angle of approximately 10^0 (<< the full angle of divergence of the X ray beam). This was done so that the active detector pixels receive a relatively uniform X ray flux.

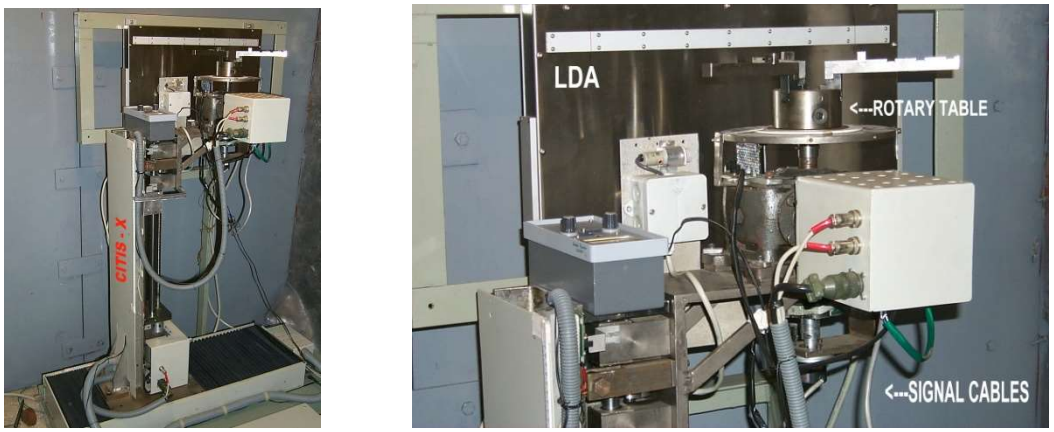

(A) **(B)**

FIG. 25 (A-B). (A) Photographic view of an X ray based experimental tomography system for industrial applications, (B) a close-up view of the sample holder and LDA

4.4.1. Scanning mechanism

As shown in the schematic diagram in figures 25 (A-B), an optical trigger device is coupled to the rotary head of the mechanical system. A programmed angular motion sequence rotates the specimen platform at constant speed. The data acquisition system receives the trigger signal at a particular angular position. The angular speed is programmed in such a way that 1600 angular views are recorded in approximately one revolution. Some correction is applied to tune the transmission data array so that the first and the last projections correspond to 0^0 and approximately 360^0 angular positions. As the number of samples in a projection is 260, angular data sets are re-sampled from the large number of views recorded to commensurate with the former. Also, the transmission data was pre-processed for minimization of resulting artifacts arising due to abnormal response of some of the detector elements.

4.5.SUGGESTED STEPS-TO FOLLOW

Generally, most of the instructions provided in the preceding section 3.5 apply here also except operating mode of the X ray based LDA. The detector array operating in relatively high flux of the X ray beam would normally be designed to give out digital numbers (12 or 14-bit standard resolution) or directly a set of 2D matrix data.

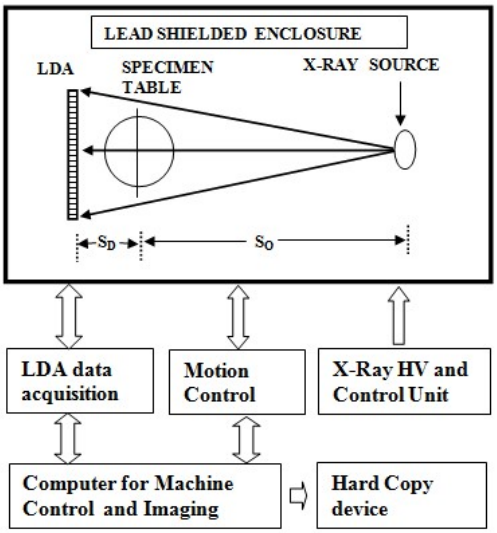

FIG. 26. Schematic diagram showing functional building blocks and geometry of the fan-beam

In some cases, the LDA may provide a frame where the LDA is normally programmed to operate in unison with a conveyor belt for online radiographic imaging (e.g. a baggage scanner).

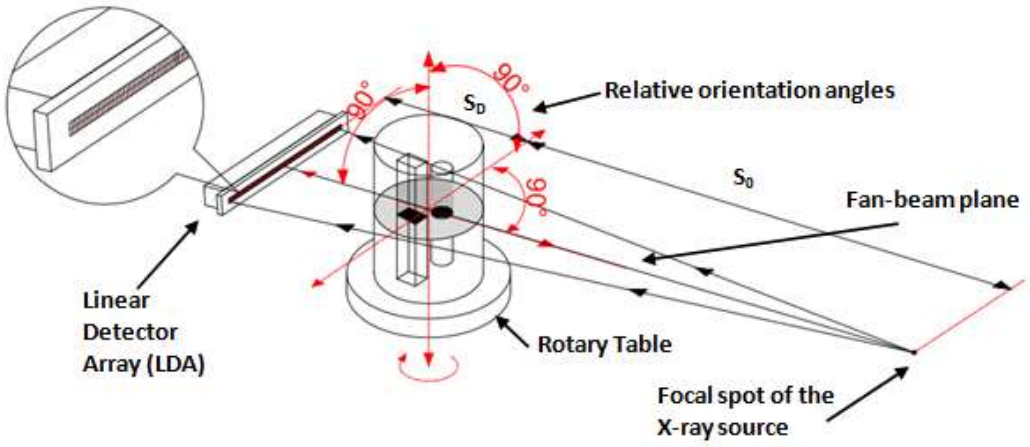

FIG. 27. Positions of the LDA, effective focal spot of the X ray source and the objects and their relative orientations

As shown in figure 26, the LDA data acquisition system, motion control and X ray control are first configured as per specific hardware design details. A central computer may possibly be able to manage all the three main sub-systems through customized machine control and data acquisition system software. Also, as shown in figure 27, the relative positions and orientation angles should be ascertained. Also, there should be no precession in the rotary axis as these errors would give rise to significantly perceptible artifacts in the reconstructed image.

The software may be easily developed as the LDA and motion controller would certainly be providing compatible high-level programming libraries. Utilizing the built-in calibration programs for the LDA, the detector array should be first calibrated for offset and gain for a given kV (anode voltage) and mA (tube current) values in the X ray control panel. The kV and mA should be fixed in such a manner that for the selected integration time of the LDA, the high flux should not be saturating the pixels. This in turn will be depending on the (S_0+S_D) distance fixed as per COR and the optimum beam angle. The scanning mechanism should be run

multiple times to see any visible instabilities or disturbances in the mechanical assemblies. Multiple frames of radiation intensities may be recorded without any object in the beam path. The data should be analyzed to check whether the offset and gain calibration performed for the set kV and mA values are effective. Specimen scanning may then be performed, and transmission data acquired and stored. If required, a digital radiograph may also be acquired by giving a synchronized movement across the vertical axis without rotating the test specimen.

The system software will be used for initiating and controlling scanning sequence and in particular would consist of computer routines for (i) programming and controlling mechanical manipulator movement, (ii) programming linear array and data transfer and (iii) pre-processing X ray measurements, image reconstruction, display and processing. In a specific scenario, as part of research and development work, the required pre-processing and image reconstruction software were developed under MS Windows operating system. The first program typically named XScanCNV-F would accept the binary data file containing raw scan data and carries out all the corrections and formatting required for tomographic image reconstruction. It also recorded information on the system geometry. The second program typically named CTRecon-F accepted output files from the XScanCNV-F software and reconstructed the tomographic image. The software had the facility to analyze the reconstructed grid values for statistical calculations and for graphical representation. The image as well as reconstructed data could then be saved in a standard format for further processing. The convolution back projection (CBP) algorithm as applied to parallel beam geometry is modified to a weighted back projection. Various algorithms as applied to tomographic image reconstruction in case of fan beam geometry can be adapted and modified to serve a particular requirement. These experimental software systems were developed some years back in the laboratory and may not be available now.

4.6.SINOGRAM CORRECTION FOR ERRORS IN SCANNING

When a tomography system is developed out of the available detector systems and mechanical manipulators as well as associated instrumentation, it is quite possible that a lack of synchronization among various sub-systems shows up in different artifacts in the reconstructed image.

4.6.1. Artefact due to lack of synchronization between rotary motion and detector data acquisition system

In industrial tomography, the X ray source and detectors are generally stationary, and the object is placed on a rotary platform. The relative motion is set to get the desired number of fan beam projections. When a rotate-only CT system operates in start-stop (steps) mode, there is definite information on the angular position for each projection since the rotary part is programmed in that way. This ensures that there is almost no error in the numerical value of the angular increment, which is passed on to the reconstruction program. In case of a hard-wired continuous-rotate system also, it may be quite possible to get actual angular positions very precisely. In a situation like the one discussed in this chapter, the LDA system receives only an initial trigger and an on-board clock mechanism directs the read-out simultaneously for all the pixels (one line at a time). The rotary speed has to be programmed in such a way that it makes exactly a complete rotation (360^0) by the time the LDA reads the last programmed line. The angular increment can be calculated based on the number of projections acquired and passed on to the reconstruction program.

The projection data recorded for CT reconstruction of a single slice is given by

$$P_{\phi}(t) = \ln\left[\frac{I_0(\phi)}{I_t(\phi)}\right] = \int_{(\phi,t)} f(x,y)ds, \tag{25}$$

Where ϕ is the projection angle, t is the distance in the detector plane from the projected rotation axis and I_t and I_0 are detected beam intensities with and without object in its path respectively. Computed tomography reconstructs the object function $f(x,y)$ from the set of projection measurements $P_{\phi}(t)$. The complete set of projection data $P_{\phi}(t)$ over N_P projections with N_S rays per projections forms the sinogram.

The discrete representation of equation (25) in case of projections acquired using a linear detector array can be given as follows:

$$P_i(n.a) = \ln\left[\frac{I_0(n.a)}{I_i(n.a)}\right] \tag{26}$$

$$\text{for } 1 \leq i \leq N_P \text{ and } 1 \leq n \leq N_S$$

Here, the index i represents the angular view number and a is the detector pitch of the linear detector array. The quantity $(n.a)$ represents the pixel location along the length of the detector array. Therefore, $I_0(n.a)$ and $I_i(n.a)$ represent the detector pixel output in absence and in presence of the object respectively. Figure 28 shows discrete $I_i(n.a)$ data in sinogram representation. As evident from the mathematics of CT image reconstruction based on filtered back projection technique, the N_S x N_P grid of projection data points should be equi-spaced. In addition, the rows corresponding to 0^0 and 360^0 angular positions should represent the same projection as also the angular increment between any two consecutive rows must be the same and equal to $2\pi/(N_P - 1)$ radian. Any deviation from these requirements will lead to artifacts in the reconstructed image. CT artefacts manifest themselves in somewhat different ways, since the CT image is numerically reconstructed from a series of measurements.

4.6.2. A statistical approach for sinogram correction

The mechanism of initiating trigger to the control unit of the linear detector array can be explained as follows: The object is mounted on the specimen platform, which is reset to zero position. The constant angular speed of the rotary axis is roughly calculated based on the scanning speed of the data acquisition system. In this experiment, the LDA was programmed for nearly 125 lines per second read-out speed. It is obvious that the angular speed of the scanning mechanism should be set in such a way that it makes one complete revolution in the same time as the LDA takes to acquire a total of 1600 lines. As the corresponding angular positions for each transmission data set is not recorded on the fly, it was observed that the error in the calculated angular increment value causes artifact in the form of radially split images [21].

This is probably because the calculated angular increment $\Delta\phi$ (radian) does not truly represent the angular separation between any two consecutive projections.

$\Delta\phi$ is expressed in terms of N_P as

$$\Delta\phi = \left[2\pi/(N_P - 1)\right] \tag{27}$$

This can be attributed to the fact that the last projection data *(N_P=1600)* does not correspond to a projection at 2π radian angular locations. As a result, reconstruction using filtered back projection method may produce artefact in the CT image.

It can be observed that the projections of the same object distribution at 0^0 and 360^0 angular positions will have similar characteristics provided there is no interference in the signal. This is however an ideal case as the signal will be corrupted by statistical and electronics noise. The correction method described here assumes that a full frame is acquired where the last line corresponds to an angular position slightly greater than 2π. Now as the frame represents over-sampled projection data, the next step is to find out index corresponding to the 2π angular positions. In order to have a uniform formulation so that the same can be implemented as part of the pre-processing sequence, the difference transmission data array is defined as,

$$I_i^{Diff}(t) = I_i(t) - I_{i=1}(t) \qquad \text{for } 1 \le i \le N_p \tag{28}$$

The last n_p ($\approx N_P/4$) projections are used to calculate the minimum of standard deviation *(σ)* in each row of the difference signal. The first minima relative to the top of the sinogram ($i=N_P$) gives the index ($N_P^{\#}$) corresponding to the 2π angular position data. The operation can be represented as

$$\sigma_{\min}\left[I_i^{Diff}(t)\right] \Rightarrow N_P^{\#}(i \equiv 2\pi) \tag{29}$$

Where

$$\sigma\left\{I_i^{Diff}(t)\right\} = \sqrt{\frac{\sum_{j=1}^{N_S}\left\{I_i^{Diff}(j) - mval_i\right\}^2}{N_S}} \tag{30}$$

With

$$mval_i = \frac{\sum_{j=1}^{N_S}\left\{I_i^{Diff}(j)\right\}}{N_S} \tag{31}$$

This leads to a value of $\Delta\phi$ as

$$\Delta\phi = 2\pi/(N_P^{\#} - 1) \tag{32}$$

In order to have another parameter to independently verify, the minimum of mean squared error (*mse)* corresponding to each row of the difference signal may also be calculated in the same way.

The index ($i = N_P^{\#}$) of the minimum of *mse* would be a pointer to the approximate 360^0 projection data. Mean squared error *mse* is defined as

$$mse_i = \frac{\sum_{j=1}^{N_S} \left\{ I_i^{Diff}(j) \right\}^2}{N_S} \tag{33}$$

The minimum of mean squared errors (*mse*) can be an indicator to two similar transmission data sets while the minimum of the standard deviation as given by eq. (30) indicates that elements of $I_i^{Diff}(j)$ differ too little from the mean value. This again implies that the two transmission data sets, which produced that particular $I_i^{Diff}(j)$ array, have too much similarity. The 0^0 and 360^0 will have the highest probability for the lowest sigma.

For tomographic reconstruction reported here, the index $N_P^{\#}$ found on the basis of minimum σ (eq. 30) was used for further processing the transmission data. This is also to be noted that slight mismatch in the rotary speed of the mechanism and the data acquisition speed may not produce visible artefact of the kind described above in case of circularly symmetric objects as all projections would be characteristically the same. Figure 28 shows a schematic diagram of the operations carried out for this purpose.

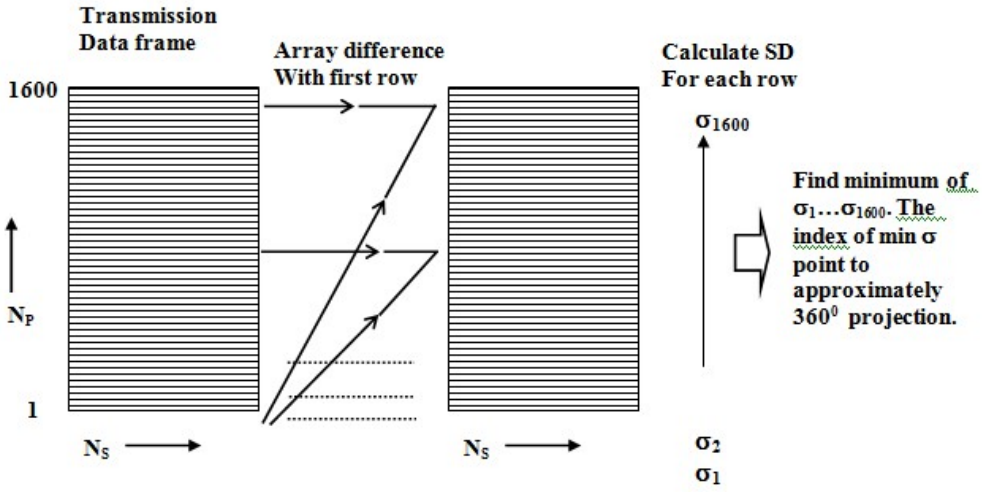

FIG. 28. Block diagram of the proposed numerical operations

A detailed discussion on implementation of this technique is not desirable here. Similarly, there is bound to have non-uniformity in the detector output even though the pixels have been calibrated at a particular kV and mA of the X ray tube. The reader is referred to published literature [22, 23] on these problems and some suggested techniques to minimize their effects on tomographic images. The corrective methods may be applied in tandem on the raw transmission data and the projection data before carrying out the reconstruction.

4.7.SOME RESULTS

Figure 29 shows pot sample # placed on the experimental X ray tomography scanner having system parameters as tabulated in Table 2. Figure 30-A is a typical radiographic view of the pot sample with a metal clip (diameter = 0.8 mm) attached at one side. At the pot exterior, there are four flower design protrusions located around its upper middle section. This radiograph clearly shows a good representation of the pot and metal clip, both in shape and contrast. The radiographic view has been generated on the same scanner by giving a synchronized vertical movement to the object. However, the flower protrusions' images are superimposed with the main body image.

FIG. 29. A test specimen is placed on the object platform.

The X ray tube is shown in the extreme right side

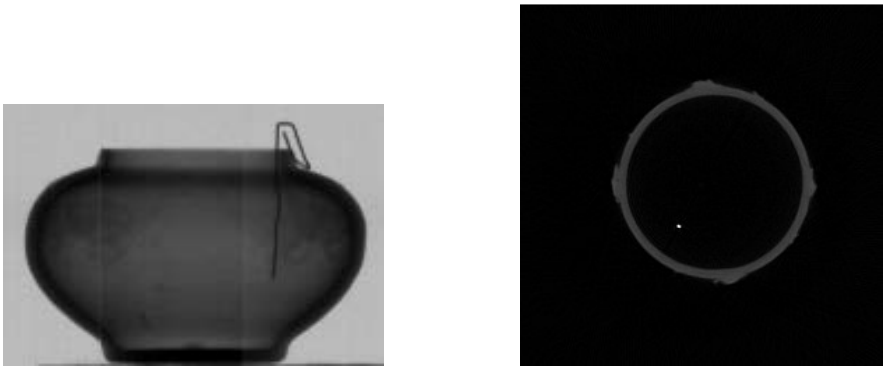

(A) (B)

FIG. 30 (A-B). The digital radiograph shows a metallic wire and some density variation across the radiograph, (B) a typical section through the test specimen in the form of a tomography. The image clearly shows the high density dot giving the wire location inside the object.

 # Experimental work in ICT by an IAEA Fellow from Malaysia deputed to India - BARC

The ICT image in figure 30-B shows the pot's round shape with near symmetrical protrusions around the pot's cross-section. The protrusions are odd-shaped flower designs moulded by the same clay material. One tiny white dot (feature) is seen in the image, which corresponds to the cross-section of the long end of the metal clip. Using the ICT software, the width and inner diameter of the pot at each section could be easily determined. The grey and white features represent the clay and metal material.

Figure 31 shows a photograph of another test specimen used in the experiment for visualising combined digital projection radiographic and computed tomographic images. A section of twelve aluminium circular tubes welded together were housed in a thin commercial thin metallic container with a seam-welded joint along its length. The maximum material thickness in the beam path was found to produce projection radiographic views with sufficient contrast to visualise the aluminium structure inside the container. The digital data obtained from the linear detector array was processed to obtain the typical radiographic image shown in figures 32 (A-B). The LDA was calibrated at an X ray tube voltage of 100 kV. The specimen was placed on the platform and it was given a vertical movement in synchronisation with the data

acquisition system. The acquired 12-bit digital data was scaled to 256 grey values for display purpose.

FIG.31. Photograph of the specimen – a commercial thin metallic container [100mm(H)x100mm (OD)] housing a section of welded aluminium curved tubes (12 nos.). The container was partially filled with water.

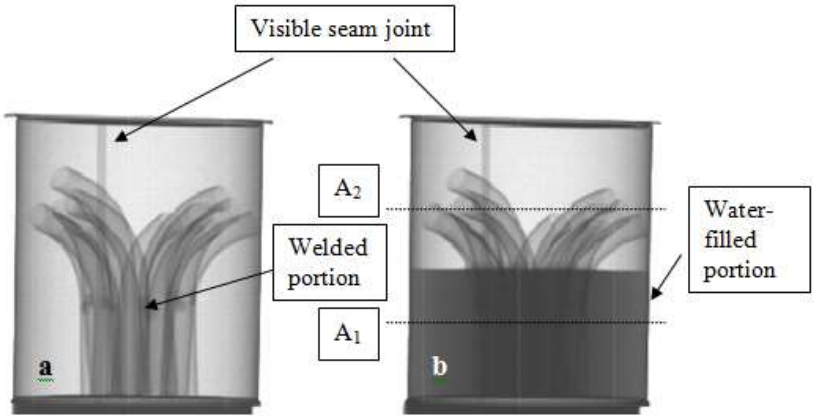

FIG. 32 (a-b). (a) radiographic view of the container assembly and (b) radiographic view of the same specimen partially filled with water at 100 kV.

Figure 32 (a-b) shows the radiographic image of the container assembly under two different conditions. The image clearly shows the inside details of the specimen where the seam joint of the container wall, change in thickness in the welded portion of the tubes structure as well as the smooth thickness gradient due to circular shape of the container.

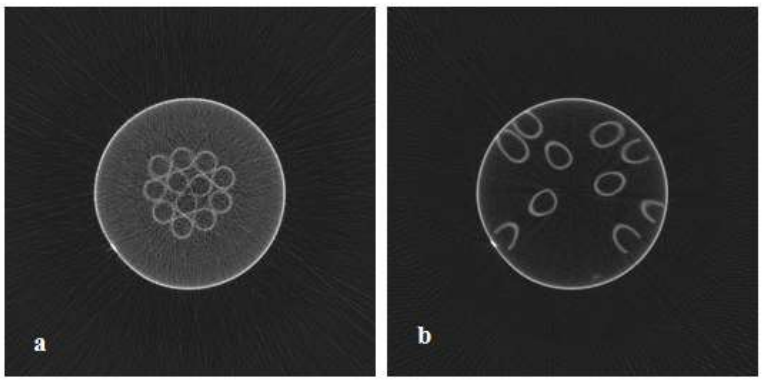

FIG. 33. Typical tomographic images of the container-assembly cross-sections marked (a) A_1 in fig. 32 (B) and (b) A_2 in fig. 32 (B) at 100 kV

Figure 32-b was obtained with the container partially filled with water. This was done to increase the material thickness in the beam path up to some height so that the contrast got reduced in that portion and almost no details are seen for the aluminium structure. This is due to the fact that the energy of the X-rays is not sufficient to record details with sufficient contrast in the given configuration. The X ray tube voltage was kept constant at 100 kV for these two images.

Figure 33a is the computed tomographic image of a typical cross-section of the specimen in the water-filled region. This is marked as level A_1 in figure 32a. It can be seen that the image distinctly shows the container's thin wall cross-section, high thickness region of the seam joint in it and the aluminium tubes' cross-section inside the water. The uniform-density water region has some grainy noise visible which is due to the limited signal to noise ratio in the input signal. This image has significant details about the internals as compared to the radiographic image in figure 32b. Figure 33b is another tomographic cross-section at a level marked A_2 above the water level. The tubes are significantly curved in this plane. This is evident from the aluminium cross-sections, which are not seen circular in shape. The selected plane has not been able to cross all the tubes and some only in parts. The relative contrast is able to distinguish all the details expected in the cross-section.

4.8.CONCLUSION

The forgoing discussion on some of the practical aspects of computed tomography using a linear detector array may help a trained scientist or engineer to set up a laboratory system for cross-sectional imaging of industrial specimen. There is however a lot of variables and operational limits of a specified set of hardware selected and therefore a typical ICT setup using a linear detector array may not be able to cater to all test specimens. An optimized combination of a suitable X ray source and a compatible linear array detector may help in designing and developing a fan-beam tomography scanner in the laboratory. The system integrator has to carefully look into possible sources of artifacts and develop a suitable software protocol.

5. ICT IMAGING USING A TYPICAL 2D DETECTOR ARRAY

5.1.INTRODUCTION

Industrial Computed Tomography (ICT) using two-dimensional (2D) detector arrays based either on direct detection or indirect detection of projection radiographic data is becoming increasingly popular and a viable option both in terms of technology and economic considerations. The current trend in 2D detection technologies is the use of a flat panel detector (FPD) in digital radiography facilities for NDT applications. Careful selection and integration of an FPD, a suitable and compatible X ray generator and a precision computer-controlled mechanical manipulator will be able to provide a cost-effective direct 3D computed tomography solution either as an upgrade of an existing digital radiography system or a custom-designed integrated imaging solution for advanced NDE requirement. Computed tomography using a cone beam may be called Cone Beam Computed Tomography (CBCT), Volume Computed Tomography (VCT), 3D Computed Tomography (3DCT) or Flat Panel Computed Tomography (FPCT).

5.2.TWO-DIMENSIONAL DETECTOR ARRAY

In the very broad sense, a two-dimensional detector system should be able to capture and record radiographic projection image of a three-dimensional object exactly as a film does. In electronic imaging, there are many conventional and modern technologies available for such requirements. However, not all direct 2D detection technologies may be suitable or feasible for ICT image reconstruction due to inherent limitations. Flat panel detectors (FPD) are a class of solid-state X ray digital radiography devices similar in principle to the image sensors used in digital photography.

Indirect detectors contain a layer of scintillator material, either gadolinium oxysulfide or caesium iodide, which converts the X-rays into light. Due to the impracticability of focusing x-rays, the sensors have exactly the same size as the image they capture. Directly behind the scintillator layer is an amorphous silicon-on glass detector array. Millions of pixels each containing a thin-film transistor form a grid patterned in amorphous silicon on the glass substrate. [1]*http://en.wikipedia.org/wiki/Flat panel detector*

Similar to a digital camera's image sensor chip, each pixel also contains a photodiode which generates an electrical signal in proportion to the light produced by the portion of scintillator layer in front of the pixel.

The signals from the photodiodes are amplified and encoded by additional electronics positioned at the edges or behind the sensor array in order to produce an accurate and sensitive digital representation of the X ray image.

Direct FPDs amorphous selenium (a-Se) FPDs are known as “direct” detectors because X ray photons are converted directly into charge. The outer layer of the flat panel in this design is typically a high-voltage bias electrode. X ray photons create electron-hole pairs in a-Se, and the transit of these electrons and holes depends on the potential of the bias voltage charge. The charge pattern is then read by a TFT array in the same way images produced by indirect detectors are read.

Direct FPDs may possibly be used only in applications involving low energy X rays. Indirect conversion FPDs may be optimised for use with a wide range of X ray energies with different types and thicknesses of the scintillator material. The image quality will however depend on many factors e.g., scintillator material and its thickness, pixel size, read-out electronics, dynamic range, specimen dimension and composition as well as the characteristics of the radiation used. The control electronics and data transfer protocol may depend on manufacturers of FPDs but are now well standardized. Normally a single personal computer may be used for controlling the operational parameters as well as receiving the actual projection data in standard image formats.

5.3.FLUOROSCOPY DETECTOR FOR RADIOGRAPHIC IMAGING

In the very basic conceptual planning for a two-dimensional (2D) X ray detector for projection radiography recording, a conventional film based system may serve the purpose. However, the requirement for multiple 2D projection images especially in electronic form for tomographic reconstruction rules out using a conventional film-based image recording method though such a system offers high resolution images. Digitising multiple films and transforming the film recording in electronic format and using the same for tomographic reconstruction is not a straightforward option as the process may have multiple sources of errors resulting in complex artefacts in the tomographic images.

Direct digitizing systems accelerate the application of intelligent procedures to facilitate and enhance image interpretation. For almost ten years, imaging plate systems have been available for NDT, and these can be used as a filmless radiography technique, also known as computed radiography with imaging plates [24]. However, such a chemical-free and relatively fast process of recording radiographic images also does not offer a viable solution for generating dimensionally accurate projections for industrial tomographic image reconstruction. Many researchers and developers have proposed and tried varied combinations of hardware in order to bring down the cost of a 2D tomographic imaging system as compared to sophisticated and commercially available configurations and still producing useful industrial CT images [25]. At the heart of such low cost tomography systems are usually a fluoroscopy or image intensifier based X ray detector system coupled with a CCD camera which helps in acquiring radiographic projection image in digital format. Development of an entry-level computed tomography system can be accomplished using a low-cost fluoroscopy based 2D digital detector [26]. However, it should be kept in mind that the quality of CT images produced by such an entry-level system may not be appealing in terms of contrast sensitivity or spatial resolution. Also, application may cater to a very limited range of industrial specimen both in terms of physical dimension and effective material thicknesses. The reader may refer to the IAEA Radiation Technology Report No. 2 (2013) on design, development and optimisation of a low cost system for digital industrial radiology.

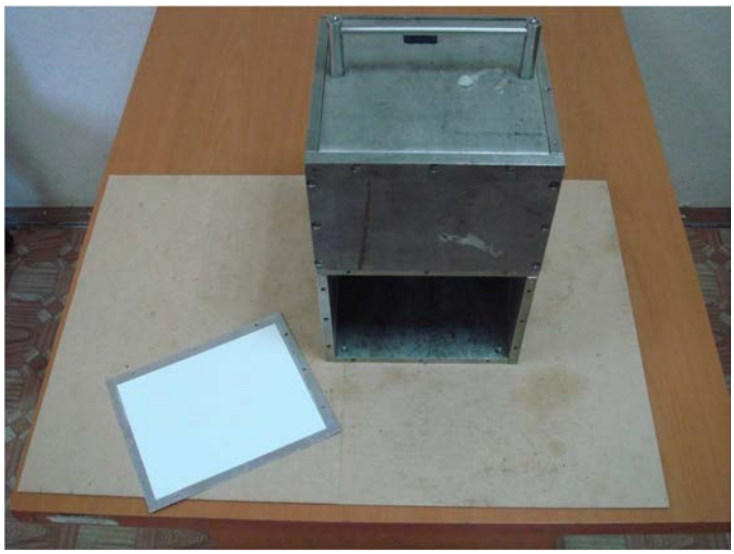

FIG.34. A typical aassembled fluoroscope and fluorescent screen developed by Germany's Federal Institute for Materials Research and Testing (BAM) (Image courtesy: IAEA Radiation Technology Report No. 2 (2013) published by International Atomic Energy Agency, Vienna)

Depending upon configuration of the fluorescent-screen and CCD based 2D digital radiographic imager, the maximum energy of the X ray radiation may be different for different systems. There may be certain situations where large and thick objects need to be radiographed or scanned for tomographic images. One such example may be non-destructive examination of 200 or 500 litre capacity waste drums. Imaging systems meant for these requirements also require high energy X rays mostly from accelerator based equipment. Alternative sizes and resolutions can be achieved by using a conventional X ray imaging system based on a scintillation screen optically coupled to a CCD camera. Using this approach, large screen X ray imagers have been commercially made available with imaging areas ranging from 25mm square to 1.0 x 1.5m. (*courtesy of* http://www.shawinspectionsystems.com/products/detectors/he%20detectors.htm).

5.4.DIGITAL DETECTOR ARRAY (DDA)

As stated earlier, one of the most modern, compact and reliable 2D digital detector array has been what is called a flat panel detector (FPD). Versatile FPDs have been in use both for radiographic applications as well as industrial tomography for almost a decade or so. Flat Panel Detectors for use in X ray based imaging applications are essentially composed of two principle imaging components. The first imaging element is a scintillator screen that converts the X rays into visible light. A wide range of scintillation screens and materials are suitable, and most manufacturers offer different screen options. This screen is directly coupled two an array of photosensitive photodiodes which convert the visible light to an electrical charge. This charge can be read out via an array of switches, of Thin Film Transistors (TFTs) and digitised. The digitised values for each photodiode, can be used to generate a corresponding grey level value in single image pixel. Thus, the array of photodiodes allows a digital radiograph to be captured directly. Each photodiode is corresponding to a pixel in the radiographic image.

The statistical fluctuations in the primary X ray beam intensity, X ray to light conversion, electronic noise and other system instabilities produce a number of false signals in the detector system. Even when the X ray beam is off, there is some noise signal generated in the imaging

hardware. Besides these, there may be gain instabilities in individual pixels. All these add up to the noise in the final image.

To quantify the effect of the noise on the actually wanted signal, the so-called signal-to-noise ratio (SNR) is defined as the ratio of the mean intensity value I_0 (signal) to the noise amplitude σ. The contrast-to-noise ratio (CNR) is defined as the ratio of the mean intensity difference between the intensities in the flaw and the surrounding material in the radiograph to the noise amplitude σ. It is common practice in defining SNR to relate the noise amplitude to the mean intensity. Large SNR implies the wanted signal, i.e. the mean intensity I_0 is large as compared to the noise. This may result in high image quality. On the other hand, a small SNR implies that the wanted signal, i.e. the mean intensity I_0 is small as compared to the noise. This may result in low image quality [27].

Contrast sensitivity and spatial resolution must be optimised as per standard guidelines before any such detector is used for radiographic or tomographic imaging applications.

5.5.GENERALIZED BLOCK DIAGRAM OF A 3D ICT SETUP

As briefed in the introduction section, an existing digital radiography setup making use of an FPD and a suitable X ray source can be upgraded to ICT setup by a system integrator who would provide technical assistance and required software support. The facility in-charge of such an existing radiography system would be required to upgrade the hardware especially the mechanical manipulator system for object rotation and alignment of the X ray source and the detector array. Figure 35 shows a typical arrangement of a direct digital radiography and computed tomography imaging facility developed around a commercially available indirect FPD, constant potential X ray generator (continuous radiation source) and a precision mechanical manipulator. The system needs to be housed inside a suitably designed radiation shielding enclosure and the imaging operations would require to be remotely controlled due to radiation safety aspects. Figure 36 shows the schematic diagram showing the relative positions of the FPD, test specimen and the X ray source on the mechanical device highlighted in the dotted section of figure 35.

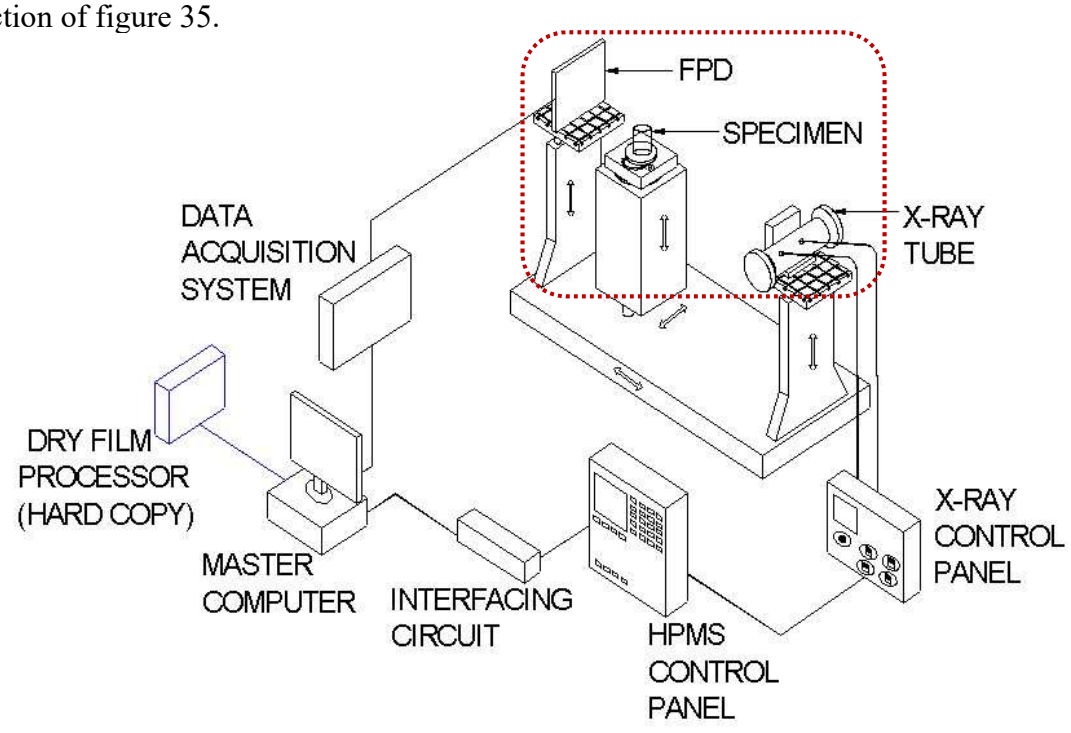

FIG. 35. Block diagram of a typical X ray based Direct Digital Radiography and Volume Tomography System

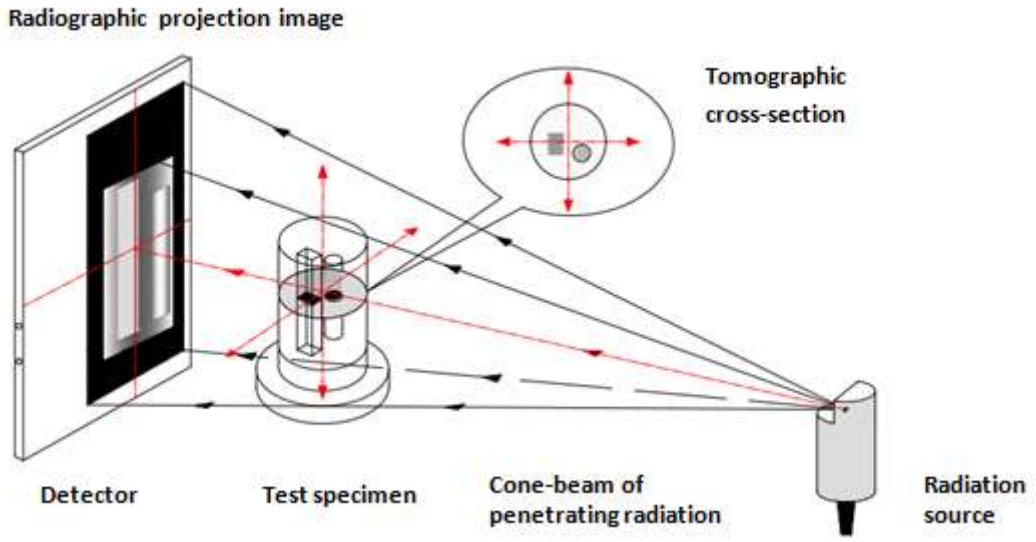

FIG. 36. Schematic diagram showing the relative positions of the FPD, test specimen and the X ray source on the mechanical device in the dotted section of figure 35.

5.6.AN EXAMPLE OF A PRACTICAL FPD BASED ICT SYSTEM

Based on the block diagram of FPD based ICT system as shown in figure 35, an integrated digital radiography and volume (direct three dimensional) imaging system was developed in the laboratory for research applications using a constant potential X ray equipment which could operate up to 420 kV of accelerating voltage and an amorphous silicon based flat panel detector (FPD) assembly as the key components. The front-end software system was developed in the laboratory, which made use of some commercial software components in the backend. Figure 37 shows a photographic view of the actual setup. At the extreme left in the picture is the 420kV X ray tube head and at the far end, the FPD assembly with a shielding plate is mounted on an alignment table. Figure 38 is the outside view of the control area in the laboratory. FPD is a fast and sensitive radiation detector and it requires exposure for a few seconds only for general imaging applications. When the system is to be used for acquisition of large number of projection data for direct 3D tomographic reconstruction, the FPD is exposed to intense X ray radiation continuously during the scanning sequence. The scanning sequence involves mechanical motion of rotary systems meant for object mounting. It has been observed that the actual exposure duration is only about 10% of the total time taken by a typical scanning sequence. Due to operational difficulties, a conventional machine based X ray generator cannot be switched on and off rapidly. The other way to restrict exposure to the FPD in such operating cycle is to use a fast-response beam shutter, which may operate automatically and in unison with the motion and data acquisition system. Figure 39-A shows the concept of a motorized lead shutter assembly designed and developed in the laboratory and figure 39-B shows the assembly mounted on the X ray head on top of a beam collimator. Figure 40 shows software interface of the master control program used to automate the scanning sequence and data acquisition.

FIG. 37. Photographic view of the X ray based Direct Digital Radiography and Volume Tomography System housed inside a shielded enclosure

FIG. 38. Control area of the X ray based Direct Digital Radiography and Volume Tomography System

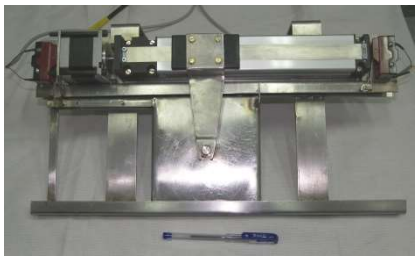

FIG. 39 (A&B). (A) Digitally controlled fast X ray shutter mechanism (B) Shutter assembly mounted on the X ray tube head on top of the beam collimator

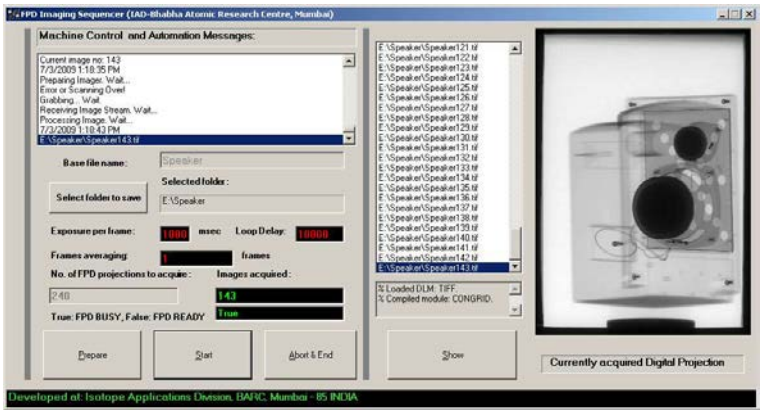

FIG. 40. Software Interface of the Master control program for the X ray based Direct Digital Radiography and Volume Tomography System

5.7.PRELIMINARY PERFORMANCE OF THE FPD BASED ICT SYSTEM

A typical FPD with 16-bit ADC hardware can provide good quality digital projection images with spatial and contrast details. The detector may have 12-bit useful resolution. The active area of the FPD used in this demonstration was roughly 4000 mm x 2800 mm. The programmed exposure can be accomplished for a variety of kV and mA combinations and the detector can be calibrated for dark current as well as beam uniformity for correct radiographic exposures. The specially developed API functions by the manufacturers were used to customize the FPD operations in an automated way. This was required as for volume tomography operations; the reconstruction software requires a large number of two-dimensional projections. A variety of pre-processing corrections are required before tomography image reconstruction using Feldkemp algorithm. The test results shown here were obtained using a commercial reconstruction software and 3D ICT data presentations were achieved using a 4GL computing environment.

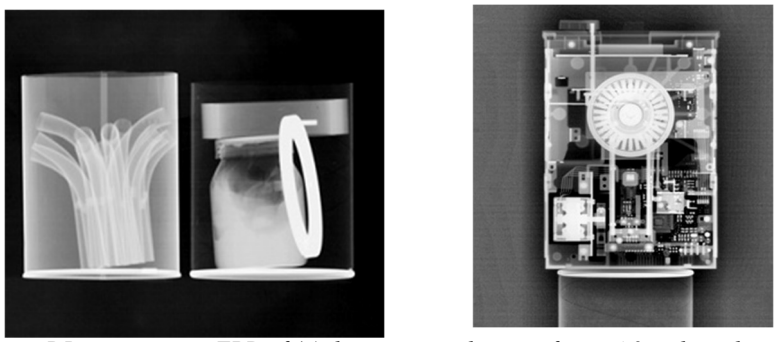

FIG. 41. Representative DR images using FPD of (a) the specimen shown in figure 4.9 and another test object showing a dried gum bottle, an adhesive tape roll and a metallic ring object (b) a 5.25" old floppy drive mechanism. These images showing spatial and contrast details have been obtained at 100-200 kV x-rays.

The test specimen used for generating ICT image data on the FPD system was a domestic electric water boiler. The test object is made up of low-density plastic material and it contains metallic components such as heating element and screws etc. The actual projection data matrix is quite large (~ 3k x 2k pixels). Tomographic reconstruction using such a large projection data-matrix requires a very large number (> 1500) of equi-angular views. This again requires a very large scanning time. It was observed that in the present configuration, time required for a single full-matrix digital projection, data transmission and mechanical movements is around 30-55 seconds. The number of angular scans was restricted to 100-200 projections and the projection matrix size was accordingly scaled down for suitable image reconstruction. The two radiographic views (figure 42) show the projection images at 0^0 and 90^0 angular positions.

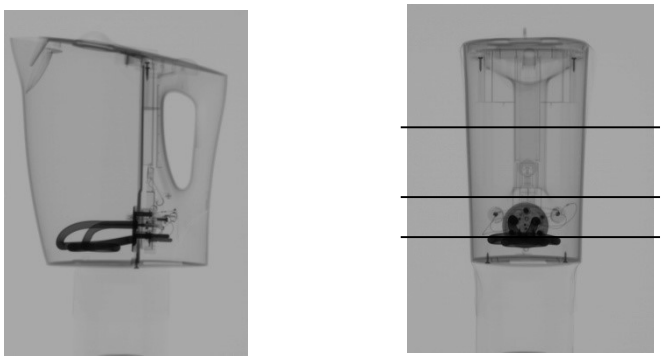

FIG. 42. Representative direct digital projection images of the test specimen as discussed in the text. The three horizontal lines in the middle picture show roughly the planes for which planar tomographic images are shown in figure 43.

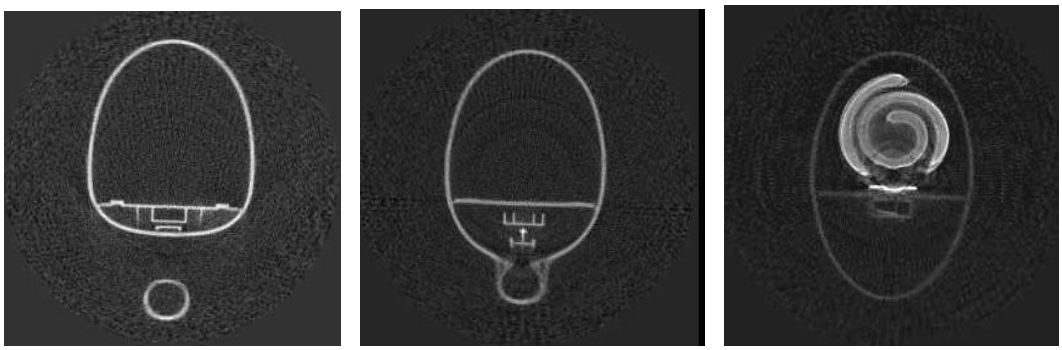

FIG 43. Representative direct digital projection images of the test specimen as discussed in the text

The three planar tomographic images shown above in the figure 43 distinctly show the internal details. The separated cross-section of the handle in the first picture, the separate water compartment in the main body and a typical cross-section of the coiled heating element is clearly visible. Figure 44 shows the extracted three-dimensional views of the heating element in two different perspective views. These images do contain reconstruction noise which can be very easily removed.

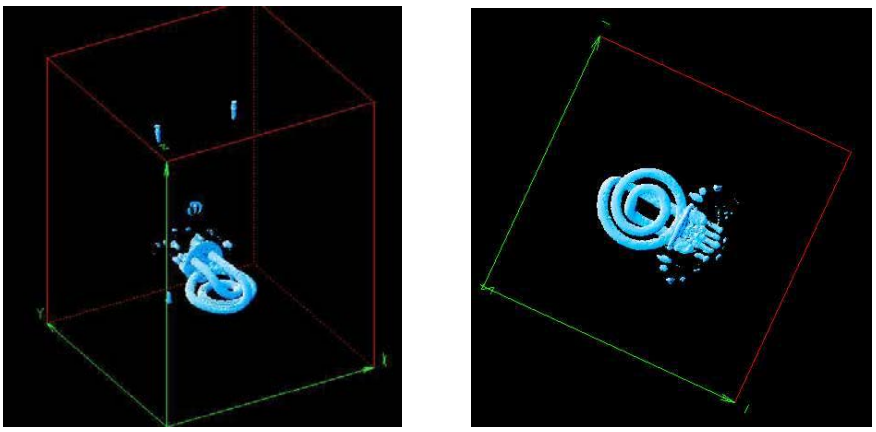

FIG. 44. Three dimensional views of the heating element in two different perspective views

5.8.CONCLUSION

It can be seen from the available published technical materials and the current trend in technologies for practical and cost effective ICT that a 2D detector array based existing digital radiography setup can be upgraded to a tomography imaging facility with the help of third-party system-integrators. Wisely selected technology facilitators may be able to advise and provide necessary hardware and software components as well as guide on important radiological issues. Due to specialized technical complexities involved in such retrofitting exercises, it is not advisable for an average user or practitioner of DIR systems to take up such exercise on his own.

6. ADVANCED CAPABILITIES OF INDUSTRIAL TOMOGRAPHY, IMPORTANT STANDARDS AND GUIDELINES

6.1.INTRODUCTION

Industrial computed tomography as an advanced NDT tool is fast evolving both in terms of technology and applications. Whenever a useful technology matures enough to be applied for direct adaptation to real world problems, it becomes inherent that many advanced applications require enhanced capabilities in the system. In addition to this, various standards and guidelines gradually take shape for the technology to be practiced in a unified and coordinated way and for which the majority of the users would mutually agree. ICT as such being a multi-disciplinary technology and, in a way, different from the conventional NDT techniques, require a user or practitioner to be conversant not only in the basic science and engineering aspects but also in the diagnostic technicalities.

6.2.ADVANCED CAPABILITIES OF INDUSTRIAL TOMOGRAPHY

The 6th conference on industrial computed tomography 2016 (iCT2016) in Wels/Austria has summarised that the application areas of CT are diverse and extensive, since any material or component can be examined with CT. The major application areas of CT in science and industry are non-destructive testing, 3D materials characterization and dimensional measurements (metrology). Some of the key uses for CT scanning are flaw detection, failure analysis, 3D analysis and material composition, extraction of material properties for finite-element simulation, fibre extraction, assembly analysis, actual/nominal comparison and reverse engineering applications. Industrial CT is used in various different industry sectors, but particularly in the automotive-, aerospace- and materials industry. A review article by Johann Castner et al. [28] has elaborated on High-resolution CT, Quantitative CT, In-situ CT, phase contrast CT and in-line CT. Many complex and advanced image processing and analysis software can be used with 3D CT data to extract information on material and structural properties of the test specimen which seemed impossible till recently. A paper by J P Kruth el al. [29] has provided status report on dimensional X ray CT measurement. It also states that the CT metrology has a high potential for dimensional quality control of components with internal cavities that are not accessible with other measuring devices. Also, CT is the only inspection process that allows combining dimensional and material quality control. The authors also indicate that CT systems might substitute other measuring and testing systems to a certain extent.

Federal Institute of Material Research and Testing (BAM), Germany has been working in the field of X ray computed tomography (CT) since more than twenty-five years and several scanners were developed from LINAC based large scale tomography down to synchrotron tomography with crack detection in the nanometer region. CT has been applied recently for dimensional measurement of industrial products, which cannot be accessed by mechanical and optical systems. The comparison with measurements of coordinate measurement machines (CMM) yields information on accuracy and tolerances. New mobile systems were developed for inspection of industrial components which cannot be brought into laboratories. Cross sections of welded pipes were measured non-destructively in primary circuits of nuclear power plants [30].

6.2.1. CT Metrology

The ability of Computed Tomography for measurement of dimensions is well known since its first application in the 70ties. Nowadays the accuracy of CT could be significantly improved, and the modern scanners can be produced in a series with relatively affordable costs. This makes the CT technology interesting as NDT and touchless measurement tool for dimensions, and especially, for inner dimensions which cannot be accessed by mechanical or optical tools. Prerequisite for the CT application is the accurate validation of the measurement procedure in comparison to coordinate measurement machines (CMM) and the present standards for determination of accuracy parameters with measurement systems. A new generation of multi sensor CMMs combines the CT operation with optical sensors and tactile probing. However, an important aspect of all coordinate measurements is the traceability of the geometry information obtained. To achieve traceability, several standards have been developed in recent years. Within this development, a VDI/VDE (Association of German Engineers) guideline has been defined, which describes how a CT system for use in 3D metrology can be qualified. (VDI/VDE 2630-1.3, 2011-12). prEN ISO 10360-11 (under drafting) is an attempt by European Committee for Standardization. The intention is to achieve comparability with the characteristics of coordinate measuring devices with tactile and with optical sensors. The characteristics described in this part serve for the specification of coordinate measuring devices with CT sensors and for a comparison between various measurement systems. Material standards with high information content are a sphere calotte plate made of zerodur and a sphere calotte cube made of titanium, which provides 2D or 3D information for CT system testing and correction, respectively. The following parameters have to be determined: Sphere distance error (SD), probing error size (PS) and probing error form (PF). This has been performed by parallel measurements of calibration objects and real test objects with high energy CT, micro CT and CMMs. Measurement differences are visualized by color coding (figure. 45).

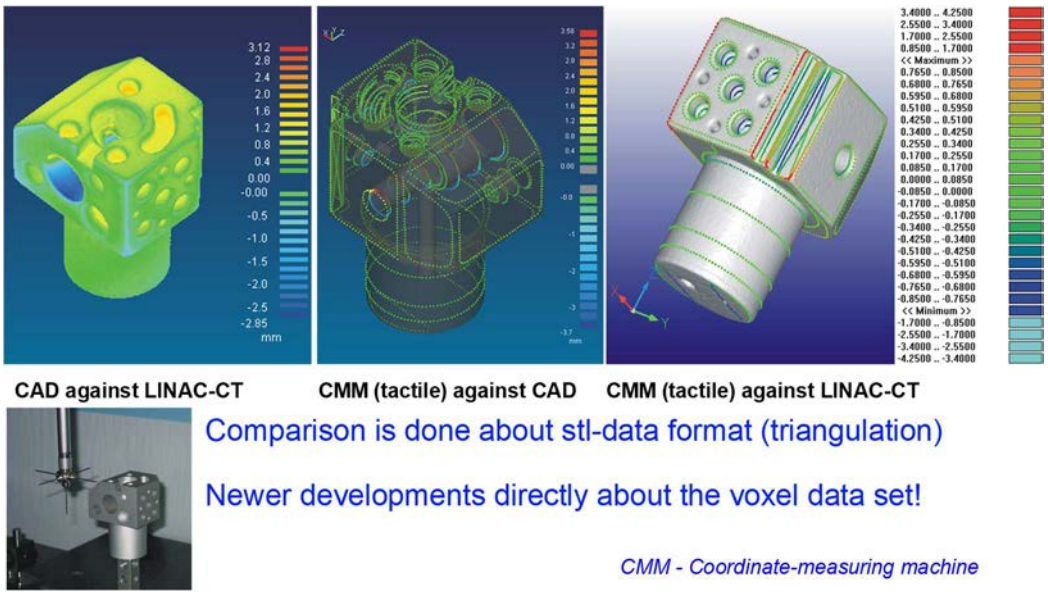

FIG. 45. Result of the comparison of the accuracy of high energy CT with a CMM measurement. The accuracies are encoded by color. (Image courtesy: Prof. U. Ewert, BAM, Germany)

6.2.2. Feature extraction by CT segmentation

Modern X-ray based industrial computed tomography imaging systems are quite robust both in terms of hardware and software capabilities. These imaging systems are capable of providing

very accurate 3D data for defect visualisation and feature extraction. The reconstruction techniques employed in generating tomographic data do introduce certain amount of noise which causes blurring of sharp edges and very fine details both in terms of dimension and physical densities. These are limiting factors of a given system and sometimes also referred to as the system capabilities. Feature extraction by CT segmentation refers to a set of mathematical processes on a given set of reconstructed CT data to isolate and obtain a specific defect or object (feature) embedded inside a large object. A typical CT segmentation process may involve filtering, quantisation and subsequent segmentation to obtain 3D boundaries of the defect or object in question. Readers may be aware that tomographic techniques can be used in process-related investigations especially in material science and chemical engineering. CT techniques may be useful in the case when non-destructive and non-intrusive observation is needed for qualitative and quantitative feature evaluation in multi-phase composites and assemblies. Porosity, which is defined as the ratio of pore volume to the total volume of the porous solid, is a physical property of porous materials and plays an important role in their mechanical and hydraulic properties of porous materials. Detailed discussion on mathematical aspects or a typical CT segmentation algorithm may be out-of-context here. However, some images related to a typical example of CT segmentation performed on an automobile part provided by Prof. U. Ewert of BAM, Germany may be sufficient to understand the importance of the technique for feature extraction in non-destructive evaluation.
Figure 46 shows a typical example. A compressor was scanned with a high-energy CT unit. The radiation source used in the scanning was a 7.5 MV Betatron and the detector was PerkinElmer PE 1620 of an area of 40 x 40 cm² having a resolution of 200 µm.

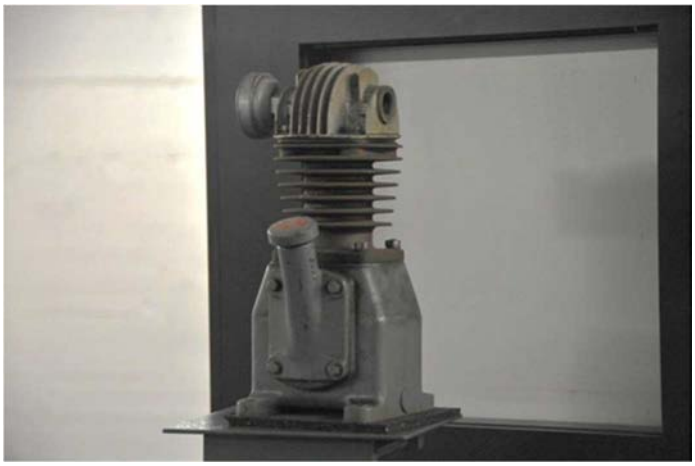

FIG. 46: Photograph of a compressor in front of a digital detector array

The CT permits the segmentation of the different parts of the compressor into different color-coded components. Figure 47a shows a central slice and figure 47b, a presentation of the complete compressor with different opacity and color of different parts. Consequently, a separated evaluation of the integrity and the inner flaws of the different parts is possible. Figure 48a shows the piston with bolt and piston rings only. The piston bolt shows marks at the position of the piston bearings as shown in figure 48b. This may be generated by the incomplete feature extraction procedure or abrasion at bearings. The feature extraction was performed with the VGStudio MAX 2.2 software from VolumeGraphics. Volumetric areas with different effective linear attenuation coefficient values can be separated and be presented in different colors. Volumetric boundaries can be considered to separate special object or features and reduce crossover. *(Image and data courtesy: U. Ewert, M. Tschaikner, BAM, Germany)*

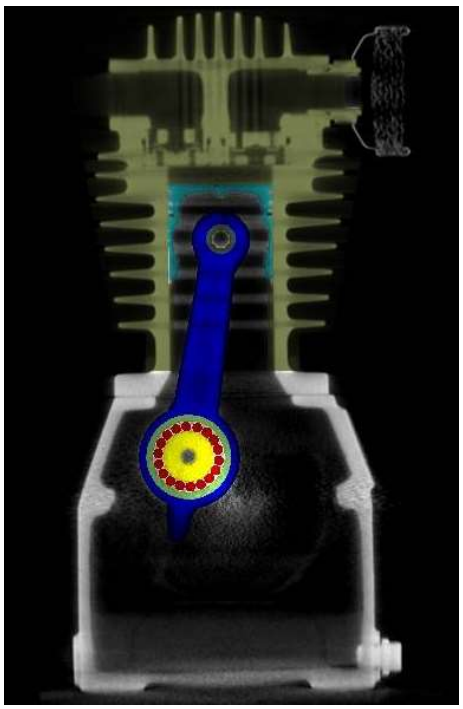

FIG. 47a: CT image with color-coded feature extraction (2D slice) taken with Betatron (7.5 MV) and DDA at SSD = 2230 mm and SOD = 1860 mm

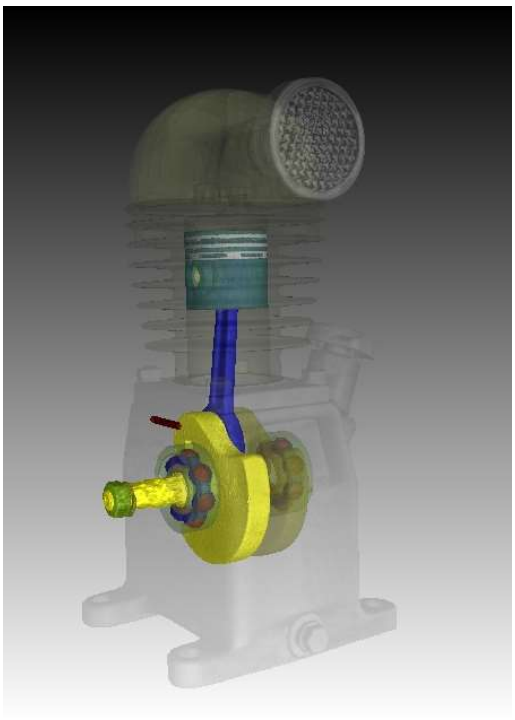

FIG. 47b: CT image with feature extraction and opaque casing and cooler block (perspective 3D presentation)

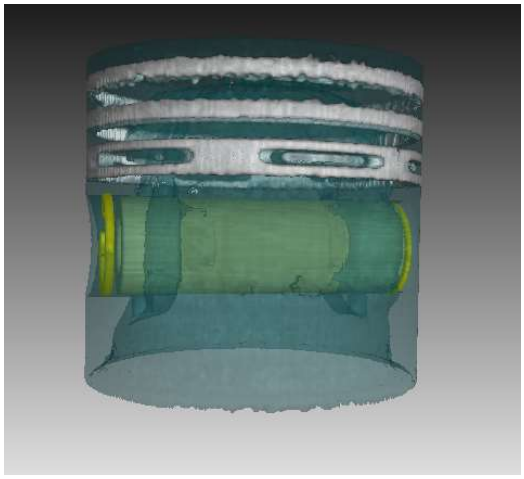

FIG. 48a: Piston with bolt and piston rings

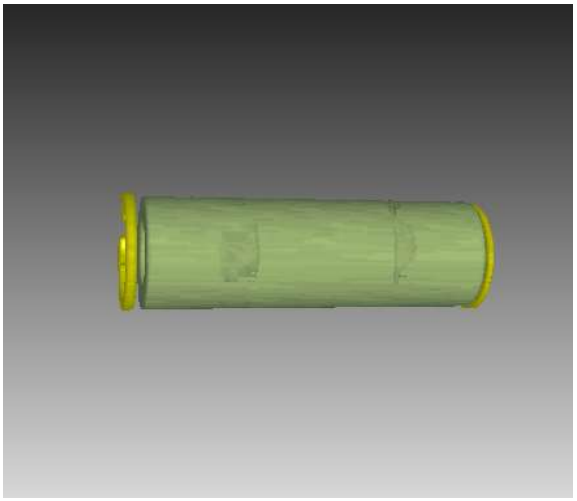

FIG. 48b: Bolt and rings with marks at the piston bolt

6.3.IMPORTANT STANDARDS AND GUIDELINES

It should be kept in mind however that guidelines issued by various agencies and professional bodies in CT but specifically meant for medical and clinical applications may not be applicable for industrial non-destructive evaluation. Prominent international bodies e.g., ASTM International, formerly known as the American Society for Testing and Materials (ASTM) and International Organization for Standardization (ISO) have published a number of significant Standard Guides and Practices for computed tomography for industrial applications. This chapter highlights some of the important documents by ASTM and ISO which are of direct relevance to ICT. *However, it should explicitly be noted that these documents must be*

purchased as per instructions of the publishers and the information provided here are taken from their respective websites as provided therein for introduction only.

6.4.ASTM GUIDELINES

6.4.1. ASTM E1441-11: Standard Guide for Computed Tomography (CT) Imaging

This guide provides a tutorial introduction to the theory and use of computed tomography. This guide begins with an overview intended for the interested reader with a general technical background. Subsequent, more technical sections describe the physical and mathematical basis of CT technology, the hardware and software requirements of CT equipment, and the fundamental measures of CT performance. Most importantly, this guide establishes consensus definitions for basic measures of CT performance, enabling purchasers and suppliers of CT systems and services to communicate unambiguously with reference to a recognized standard. This guide also provides a few carefully selected equations relating measures of CT performance to key system parameters.

6.4.2. ASTM E1570-11: Standard Practice for Computed Tomographic (CT) Examination

The document deals with the practice which is applicable for the systematic assessment of the internal structure of a material or assembly using CT technology. This document may be used for review by system operators, or to prescribe operating procedures for new or routine test objects.

This also provides the basis for the formation of a program for quality control and its continuation through calibration, standardization, reference samples, inspection plans, and procedures.

6.4.3. ASTM E1672-12: Standard Guide for Computed Tomography (CT) System Selection

This document covers guidelines for translating application requirements into computed tomography (CT) system requirements/specifications and establishes a common terminology to guide both purchaser and supplier in the CT system selection process. This guide is applicable to the purchaser of both CT systems and scan services. Computed tomography systems are complex instruments, consisting of many components that must correctly interact in order to yield images that repeatedly reproduce satisfactory examination results. Computed tomography system purchasers are generally concerned with application requirements. Computed tomography system suppliers are generally concerned with the system component selection to meet the purchaser's performance requirements. This guide is not intended to be limiting or restrictive, but rather to address the relationships between application requirements and performance specifications that must be understood and considered for proper CT system selection.

6.4.4. ASTM E1695-95(2013): Standard Test Method for Measurement of Computed Tomography (CT) System Performance

Two factors affecting the quality of a CT image are geometrical unsharpness and random noise. Geometrical unsharpness limits the spatial resolution of a CT system, that is, its ability to image fine structural detail in an object. Random noise limits the contrast sensitivity of a CT system, that is, its ability to detect the presence or absence of features in an object. Spatial resolution

and contrast sensitivity may be measured in various ways. ASTM specifies spatial resolution be quantified in terms of the modulation transfer function (MTF) and contrast sensitivity be quantified in terms of the contrast discrimination function (CDF) (Guide E1441 and Practice E1570). This test method allows the purchaser or the provider of CT systems or services, or both, to measure and specify spatial resolution and contrast sensitivity.

6.4.5. ASTM E1814-14: Standard Practice for Computed Tomographic (CT) Examination of Castings

This practice covers a uniform procedure for the examination of castings by the computed tomography (CT) technique. The requirements expressed in this practice are intended to control the quality of the non-destructive examination by CT and are not intended for controlling the acceptability or quality of the castings. This practice implicitly suggests the use of penetrating radiation, specifically X-rays and gamma rays.

This practice provides a uniform procedure for a CT examination of castings for one or more of the following purposes:

- Examining for discontinuities, such as porosity, inclusions, cracks, and shrink;
- Performing metrological measurements and determining dimensional conformance; and
- Determining reverse engineering data, that is creating computer-aided design (CAD) data files.

6.4.6. ASTM E1935-97(2013): Standard Test Method for Calibrating and Measuring CT Density

This test method covers instruction for determining the density calibration of X- and γ-ray computed tomography (CT) systems and for using this information to measure material densities from CT images. The calibration is based on an examination of the CT image of a disk of material with embedded specimens of known composition and density. The measured mean CT values of the known standards are determined from an analysis of the image, and their linear attenuation coefficients are determined by multiplying their measured physical density by their published mass attenuation coefficient. The density calibration is performed by applying a linear regression to the data. Once calibrated, the linear attenuation coefficient of an unknown feature in an image can be measured from a determination of its mean CT value. Its density can then be extracted from knowledge of its mass attenuation coefficient, or one representative of the feature.

6.4.7. ASTM E 1931-09 Standard Guide for X ray Compton Scatter Tomography

ASTM E 1931-09**: t**his guide covers a tutorial introduction to familiarize the reader with the operational capabilities and limitations inherent in X ray Compton Scatter Tomography (CST). Also included is a brief description of the physics and typical hardware configuration for CST. The principal advantage of CST is the ability to perform three-dimensional X ray examination without the requirement for access to the back side of the examination object. CST offers the possibility to perform X ray examination that is not possible by any other method. The CST sub-surface slice image is minimally affected by examination object features outside the plane of examination. The result is a radioscopic image that contains information primarily from the

slice plane. However, as with any Non-Destructive Testing method, CST has its limitations. The technique is useful on reasonably thick sections of low-density materials.

6.5.ISO STANDARDS

6.5.1. ISO 15708-1:2002

ISO 15708-1 provides a tutorial introduction to the theory and use of computed tomography. This part of ISO 15708 includes an extensive glossary (with discussions) of CT terminology and an extensive list of references to more technical publications on the subject. Most importantly, this part of ISO 15708 establishes consensus definitions for basic measures of CT performance, enabling purchasers and suppliers of CT systems and services to communicate unambiguously with reference to a recognized standard. It also provides a few carefully selected equations relating measures of CT performance to key system parameters.

ISO 15708-1 gives guidelines for and defines terms for addressing the general principles of X ray CT as they apply to industrial imaging. It also gives guidelines for a consistent set of CT performance parameter definitions, including how these performance parameters relate to CT system specifications.

6.5.2. ISO 15708-2:2002

ISO 15708-2 describes CT procedures that can provide for non-destructive testing and evaluation. Requirements in this part of ISO 15708 are intended to control the reliability and quality of the CT images. This part of ISO 15708 is applicable for the systematic assessment of the internal structure of a material or assembly and may be used to prescribe operating CT procedures. It also provides a basis for the formation of a programme for quality control and its continuation through calibration, standardization, reference samples, inspection plans and procedures.

ISO 15708-2 gives guidelines for procedures for performing CT examinations. It is intended to address the general use of CT technology and thereby facilitate its use. This part of ISO 15708 implicitly assumes the use of penetrating radiation, specifically X ray and gamma ray.

6.6.EUROPEAN COMMITTEE FOR STANDARDIZATION (CEN) STANDARDS AND GUIDELINES

6.6.1. EN 16016-1:2011

The European Standard EN 16016-1:2011 defines terms used in the field of tomography. This European Standard contains not only tomography-specific terms but also other more generic terms spanning imaging and radiography. The definitions for some of these terms feature a discussion point to refocus the term in the more specific context of computed tomography.

6.6.2. EN 16016-2:2011

The European Standard EN 16016-2:2011 specifies the general principles of computed tomography (CT), the equipment used and basic considerations of sample, materials and geometry.

6.6.3. EN 16016-3:2011

The Standard EN 16016-3:2011specifies an outline of the operation of a CT system, and the interpretation of the results in order to provide the user with technical information to select suitable parameters.

6.6.4. EN 16016-4:2011

This Standard EN 16016-4:2011specifies guidelines for the qualification of the performance of a CT system with respect to various inspection tasks.

6.7.VDI/VDE SOCIETY FOR METROLOGY AND AUTOMATION ENGINEERING GUIDELINES

The technical committee on computed tomography in dimensional metrology has prepared guidelines VDI/VDE 2630 PART 1.1 TO 1.4. The purpose has been to outline conditions and methods that ensure comparability and traceability of measurements.

7. ADDITIONAL INFORMATION

7.1.SOFTWARE SYSTEM FOR ICT

Industrial computed tomography is an indirect imaging method. Due to this, ICT would require an appropriate selection and application of a numerical reconstruction algorithm suitable for a particular hardware configuration. The preceding chapters of this technical guidebook have dealt with some of the fundamental theoretical and practical aspects of some of the simple configurations of ICT. It is expected that the relative merits and demerits of these practical and realizable scanning devices may guide trained personnel to arrive at an optimum solution based on cost, need and uses. Software system of ICT forms an important part of the overall resources required for realization of a tomography facility. Here some educational and commercially available software are discussed based on information available from respective developers and their websites for general awareness among the interested readers.

7.1.1. Software for simulation and rt image processing

ARTist: The *aRTist* program is a software tool for computer simulation of film and digital radiography developed by BAM, Germany. It generates synthetic radiographs based on a three-dimensional virtual setup with respect to a wide range of radiographic parameters. Over the years the BAM radiographic simulator has been developed from a laboratory application, running on dedicated hardware, to a user-friendly PC program which fulfils practical industrial requirements and can be applied for inspection planning as well. It is understood that there are some CT simulation modules also available.

CTSim: Computed Tomography is the technique of estimating the interior of objects from the measurements of radiation projected through the object. That radiation can be transmitted through the object such as in X ray computed tomography or emitted from internal radiation sources as in nuclear medicine scans. CTSim simulates the transmission of X-rays through phantom objects. These X ray data are called projections; CTSim reconstructs the original phantom image from the projections using a variety of algorithms. The program also has a wide array of image analysis and image processing functions.

Isee! And Isee! Professional software: *ISee!* (often abbreviated as *IC*) is a software which is developed for the purpose of radiographic image analysis under Microsoft Windows operation system. *ISee!* is not just another image viewer but the main purpose is analysis, i.e. various measurements, and documentation of high resolution images with high bits-depth usually arising in scientific and industrial digital imaging and digital industrial radiology in particular. *ISee! Professional* marketed by Vision in X industrial imaging GmbH develops and sells innovative X ray inspection software as well as complete NDT systems. This is the third generation of the software for industrial radiology targeted at the industrial user and designed to increase reliability, flexibility and efficiency of radiographic testing. One of the key properties of *ISee! Professional* is its neutrality and independence from hardware manufacturers. With this software, it may be possible to acquire and analyse images from different DDA detectors, CR-readers and film digitizers using exactly the same software. *ISee! Professional* is supplied with a concise set of application-optimized tools proven in over a decade of practice and which are easy to understand and to use.

CIVA: CIVA is a multi-technique (Ultrasound, Eddy Current, Radiography etc) software platform developed by the CEA LIST and its partners. CIVA is a modules package for Ultrasound Testing (UT), Eddy Current (ET), Radiography testing (RT) and Computed Tomography (CT). The CIVA platform not only provides simulation tools, but it is now also a powerful software for the analysis of your UT acquisition data. The RT simulation module allows simulating a radiographic control by taking into account the different radiation produced by X or gamma ray sources. From the simplicity of handling the CIVA interface, the user can easily and quickly set-up its configuration: Selection of the part to be inspected, definition and positioning of the source and the detector, insertion one or several flaws, definition of calculation options. Reader may like to visit the website at http://www.extende.com/radiographic-testing-with-civa for exploring more about CIVA software package on X ray and gamma ray based radiographic testing including module on industrial computed tomography.

7.1.2. Software for detector calibration and optimization

As stated earlier, most of commercially available LDAs and DDAs including FPDs come with customised detector calibration and optimization software systems. These are under normal working conditions are very effective in producing useful data for radiographic and tomographic applications. However, there are some other software programs available which may be able to tackle specific problems related to calibration and optimization of electronic data.

V2 Software from BAM: *V2* is still image acquisition software able to perform real time frame averaging of video streams, pixel correction (spatial and temporal), saving the result as a standard 16-bit grey-level TIFF image and several bits more. It is very usefully for acquisition of images from fluoroscopes or other devices like image intensifiers which produce frame- or video-streams of low SNR. Frame averaging allows to increase the SNR significantly and to see things you have never seen before The V2.exe application uses standard Windows video streams via DirectShow and ActiveX. In this way a wide range of video devices with live data streams are supported.

7.1.3. Important components of ICT software system

A general agreement may be arrived at by looking at the technical requirements of the overall software functionalities in an ICT setup. A typical computed tomography system may have (i) a physical hardware based scanning mechanism including a radiation source and a detector (ii) a nucleonic data acquisition system (iii) image reconstruction and (iv) image visualisation, measurement and analysis platform. Broadly speaking, the mechanical scanning mechanism will be a precision computer-controlled device and the nucleonic data acquisition system will also require use of a computer as very large amount of data will be needed to be acquired. Data pre-processing, image reconstruction, display and analysis system may an entirely conventional software based system running on a personal computer. In case of an FPD based ICT involving processing of very large amount of input data, the reconstruction may be carried out on software system which is dependent on some special purpose hardware boards e.g. a graphical processing unit (GPU). A general-purpose graphical processing unit (GPGPU) can also be used for development of image reconstruction software to accelerate the reconstruction process. However, these may be useful only when fast throughput of ICT images is required and may provide a cost-effective solution only in case the scanning speed is fast enough to justify a fast reconstruction.

7.1.4. Hardware control of the ICT scanning mechanism

As it is very much evident, there are numerous possibilities of realizing a mechanical scanning mechanism which is precise, caters to the proposed scanning sequence and conforms to required specifications, codes and standards. Mechanical drives in such a device may be open-loop or closed-loop controlled and possibly stepper-motor driven in a cost-effective solution. It may also be possible to develop a simple scanning device based on locally available stand-alone building blocks such as single axis drives (linear and rotary) and PC based motional controllers. Most of such PC based motional controllers come with programming support and software systems. The radiation sources can either be a sealed radioisotope source or a machine based X ray generator. The X ray equipment which may be either a pulsed-type or a constant-potential type and the same may have its own dedicated controller. Newer X ray equipment normally has a PC interface also so that the general operating parameters can be programmed directly through a computer bypassing the dedicated controller. The instantaneous status can also be monitored through the computer itself. Nuclear detectors, associated electronics and data acquisition modules may also have a dedicated controller with the option of personal computer interface. There are standard nucleonic data acquisitions systems which may be adapted for single detector ICT configuration. Multi-detector configuration or adapting an LDA or FPD may also be not-so-difficult as most of these detector arrays come with basic building blocks and software support for customization.

It may not be possible to list sources and suppliers of all such hardware sub-systems as most of these are country specific and localised except supplies from some global entities. The available web-resources may easily be explored for these purposes.

7.1.5. ICT reconstruction, display and analysis software

The tomographic image reconstruction is one of the core areas which makes ICT a different NDT tool and possible a not-so-easily realizable solution by an average user. However, for a nuclear laboratory having expertise in nucleonic electronics and computer programming, it may possibly be not a non-achievable task at least in case of the simplest single-detector tomographic scanner. If the ICT paradigm is well-understood, a trained scientist or engineering with

programming skills may be able to develop basic reconstruction software based on standard algorithms. What is important in this process is the understanding of the data structure and flow and evolving a standard procedure for the same even if there is no scope of implementing DICONDE standards at this stage. Digital Imaging and Communication in Non-Destructive Evaluation (DICONDE) is an evolving standard that provides a way for Non-Destructive evaluation (NDE) manufacturers and users to share image data. Conventional programming environments or a high-level 4GL (fourth generation programming languages) can be used to develop a usable module for CT image reconstruction.

MATLAB is a very popular and robust high language and interactive environment which provides some built-in functions for tomographic reconstructions. Various user codes and help files available may be useful and adaptable to specific user needs but not for commercial grade solution. One can also find many software codes and programs which may possibly be directly instable on a personal computer under open license also.

A web search may yield useful information on some of the available educational and commercial tomography software systems. A few of them are listed below just for representation purpose and with the sole aim of guiding the readers to look into more information on possibly many other similar software systems. It is explicitly mentioned that this is no way a comprehensive list nor it is intended to be a recommendation of any sort.

OSCaR (Open Source Cone-beam Reconstructor) appears to be a software package developed for computing three-dimensional reconstructions from data gathered from cone-beam X rayCT scanning geometries. The package is implemented in MATLAB with the intention of being easy to use and portable across many computer architectures. The code is intended for research use, not clinical or commercial implementation.

The commercially available CT reconstruction software Octopus, now further developed and distributed by a spin-off company *Inside Matters*, was originally developed by the Radiation Physics (RP) Group at the Centre for X ray tomography of the Ghent University (UGCT). The package was initially developed for the reconstruction of parallel beam geometry CT images. It appears to be one of the versatile and practical tomography reconstruction software for processing of data in almost any geometry.

Eigenor 3D X ray reconstruction (Eigenor Corporation, Finland) is a software-only solution that uses advanced algorithms. Even existing equipment can be upgraded with the software minimizing the need for expensive investments in hardware. In industrial applications, this means faster inspection and smooth production processes.

DigiXCT (X ray Computed Tomography) from Digisens (Digisens R&D, France) is a dedicated software suite for X ray tomography for non-destructive testing, reverse engineering and measurement.

CT software efxCT (North Star Imaging Inc.) is claimed to be the easiest, fastest and most complete 3D industrial CT software by the company. It appears to have many features as listed on its website.

7.2.ADVANCED FUNCTIONALITIES

For advanced processing and analysis of CT data for surface and volume rendering, image segmentation, feature extraction and animation, there are some significant software systems

commercially available. GE (GE sensing & inspection technologies) has also made available computed tomography (CT) software for fully automated industrial CT failure analysis and precision 3D metrology.

VGStudio MAX 3.0 from Volume Graphics is the latest version of the high-end software for the visualization and analysis of industrial computed tomography (CT) data. As per details available on the company's homepage, the software meets requirements for a future-proof solution for non-destructive testing. With Volume Graphics software, one can analyze and visualize industrial computed tomography (CT) data. The software offers a wide range of practical features. Thousands of companies worldwide are understood to use this product to analyze, inspect, and measure objects – in research, production, and quality assurance.

7.3. A FEW SUGGESTED WEB LINKS

It is important to note that most of the software products available commercially are regularly updated and revised. The details including access to their respective websites provided here were available at the time of compiling the details.

http://www.artist.bam.de/en/index.htm
http://www-civa.cea.fr/en/
http://www.dir.bam.de/ic/
http://www.dir.bam.de/v2/index.html
http://www.ctsim.org/
http://www.insidematters.eu/octopus/octopus-reconstruction
https://www.eigenor.com/products/x-ray-tomography/industrial
http://www.digisens3d.com/en/tomography-software/3-12-X_ray_Computed_Tomography_for_industrial_applications.html
http://www.digisens3d.com/en/soft/3-Digi_XCT.html
http://4nsi.com/software/efx-ct
http://www.ge-mcs.com/pt/news-and-press/tech-alerts/3211-ge-introduces-new-computed-tomography-ct-software-for-fully-automated-industrial-ct-failure-analysis-and-precision-3d-metrology.html
http://www.fei.com/software/avizo-3d-for-industrial-inspection/
http://www.volumegraphics.com/en/news/detail/detailansicht/vgstudio-max-30-beta/

ABBREVIATIONS

ASTM	ASTM International / American Society for Testing and Metals
CR	Computed Radiography
CRP	Coordinated Research Project
CT	Computed Tomography
DIR	Digital Industrial Radiography
DR	Digital Radiography
FPD	Flat Panel Detector (array)
IAEA	International Atomic Energy Agency
ICT	Industrial Computed Tomography
ISO	International Organization for Standardization
LDA	Linear Detector Array
LSF	Line Spread Function
MTF	Modulation Transfer Function
NDE	Non-destructive Examination/Evaluation
NDT	Non-destructive Testing
PMT	Photo Multiplier Tube
PSF	Point Spread Function
RCA	Regional Cooperation Agreement – Asia Pacific Region
RT	Radiography Testing
TC	Technical Cooperation

REFERENCES

[1] Martz H. E., Azevedo S. G., Brase J. M., Waltjen K. E. and Schneberk, "Computed tomography systems and their industrial applications", Appl. Radiat. Isot., Vol. 41, No. 10,11, pp. 943-961 (1990)

[2] George A Hay, "X ray imaging", J. Phys. E: Sci. Instrum., Vol 11, pp. 377 (1978)

[3] Rika Baba, Yasutaka Konno, Ken Ueda and Shigeyuki Ikeda, "Comparison of flat-panel detector and image-intensifier detector for cone-beam CT", Computerized Medical Imaging and Graphics, Vol. 26, Issue 3, pp. 153-158 (2002)

[4] Kak A C and Malcolm Slaney, Principles of Computerized Tomographic Imaging, USA (IEEE Press) (1988)

[5] Kypros Kouris, Nicholas M. Spyrou, Daphne F. Jackson, "Imaging with ionising radiations, Vol 1", Surrey Univ. Press (1982)

[6] Brooks Rodney A. and Di Chiro Giovanni, "Principles of Computer Assisted Tomography in Radiographic and Radioisotopic Imaging", Phys. Med. Biol., Vol. 21, No. 5, pp. 689-732 (1976)

[7] Wells P., Fillingham N., and Cramond A., "A study of errors due to reconstruction filters in computed tomography", Res. Nondestr. Eval., Vol. 8, pp. 149-163 (1996)

[8] Ramachandran G. N. and Lakshminarayanan A. V., "Three dimensional reconstructions from radiographs and electron micrographs: Application of convolution instead of Fourier Transform", Proc. Nat. Acad. Sci., Vol. 68, pp. 2236-2240 (1971)

[9] Reimers P., Goebbels J., Weise H. P., Wilding K., "Some aspects of industrial non-destructive evaluation by X rayand γ-ray computed tomography", Nucl. Instrum. Meth. in Phys. Res., Vol. 221, pp. 201-206 (1984)

[10] Gilboy W. B., "X rayand γ-ray tomography in NDE applications", Nucl. Instrum. Meth. in Phys. Res., Vol. 221, pp. 193 (1984)

[11] ASTM INTERNATIONAL, E1441-11 Standard Guide for Computed Tomography (CT) Imaging, ASTM International (2011)

[12] Brooks Rodney A.and Di Chiro Giovanni, "Statistical limitations in X rayreconstructive tomography", Med. Phys., Vol. 3, No. 4, pp. 237-240 (1976)

[13] Munshi P., Rathore R. K. S., Ram K. S. and Kalra M. S.,"Error estimates for tomographic inversion", Inverse Problems, Vol. 7, pp. 399-408 (1991)

[14] Schneiders Nicholas J. and Bushong Stewart C., 'Single step calculation of the MTF from the ERF', Med. Phys., Vol. 5(1) (1978)

[15] Rapaport M. S., Gayer A., "Application of gamma ray computed tomography to non-destructive testing", NDT&E International, Vol. 24, No. 3, pp. 141-144 (1991)

[16] Shepp, L. A., Hilal, S. K., Schulz, R. A., "The tuning Fork Artifact in Reconstruction Tomography", Computer Graphics and Image Processing, Vol. 10, pp. 246-255 (1979)

[17] Umesh Kumar, G. S. Ramakrishna, S. S. Datta and V. R. Ravindran, "Prototype gamma-ray computed tomographic imaging system for industrial applications", Insight (The British Journal of NDT), Vol. 42, No. 10, pp. 662-666 (2000)

[18] Kowalski G., "Reconstruction of objects from their projections – the influence of measurement errors on the reconstruction", IEEE Trans. Nucl. Sc., Vol. NS-24, No. 1, pp. 850-864 (1977a)

[19] Kowalski G., "The influence of fixed errors of a detector array on the reconstruction of objects from their projections", IEEE Trans. Nucl. Sc., Vol. NS-24, No. 5, pp. 2006-2016 (1977b)

[20] Duerinckx Andre J. and Macovaski Albert,"Classification of artefacts in X rayCT images due to non-linear shadows", IEEE Trans Nucl. Sc., Vol. NS-26, No. 2, pp. 2848-2852 (1979)

[21] Umesh Kumar, A. S. Pendharkar, G. S. Ramakrishna, S. Kailas, "A statistical correction method for minimization of systemic artifact in a continuous-rotate X raybased industrial CT system", Nucl. Instr. Meth. in Phy. Res. A, 515, 829–839 (2003)

[22] Umesh Kumar, G. S. Ramakrishna, "A mixed approach to artifacts minimization in a continuous-rotate X raybased tomographic imaging system using linear detector array", Appl. Radiat. Isot., Vol. 57, Issue 4, pp. 543-555 (2002b)

[23] Umesh Kumar, G. S. Ramakrishna, A. S. Pendharkar, Gursharan Singh, "Behaviour of reconstructed attenuation values with varying X raytube voltage in an experimental third-generation industrial CT system using linear detector array", Nucl. Instr. Meth. in Phy. Res. A., 490, Issue 1-2, pp. 379-391 (2002c)

[24] INTERNATIONAL ATOMIC ENERGY AGENCY (IAEA) Radiation technology Reports No. 2, Design, development and optimization of a low cost system for digital industrial radiology, IAEA, Vienna (2013)

[25] Andrew A. MALCOLM, Seaw Jia LIEW, Tong LIU, Ting Ying JIANG, "Enhanced Affordable Computed Tomography Solutions", 2nd International Symposium on NDT in Aerospace 2010 - We.1. A.1

[26] Andrew A. MALCOLM, Seaw Jia LIEW, Tong LIU, Ting Ying JIANG, "Development of Entry-level Computed Tomography Systems", SINCE2011, Singapore International NDT Conference & Exhibition , 3-4 November 2011

[27] U. Ewert et al., Lecture Volume of the IAEA/RCA Regional Training Course on Digital Industrial Radiology and Computed Tomography Applications in Industry Kajang, Malaysia, 2 – 6 November 2009

[28] Johann KASTNER, Bernhard PLANK and Christoph HEINZL, “Advanced X ray computed tomography methods: High resolution CT, quantitative CT, 4DCT and phase contrast CT”, Digital Industrial Radiology and Computed Tomography (DIR 2015) 22-25 June 2015, Belgium, (www.ndt.net/app.DIR2015)

[29] J.P. Kruth et al, Computed tomography for dimensional metrology; CIRP Annals - Manufacturing Technology 60 (2011) 821–842

[30] Uwe Ewert, Computed Tomography at BAM –From High Energy Technique to nm Scale, BAM, Federal Institute for Materials Research and Testing, Unter den Eichen 87, 12205 Berlin, Germany; Proc. NDE 2009, December 10-12, 2009)

BIBLIOGRAPHY

ASTM INTERNATIONAL, E1570-11: Standard Practice for Computed Tomographic (CT) Examination, ASTM International (2011)

ASTM INTERNATIONAL, E1672-12: Standard Guide for Computed Tomography (CT) System Selection, ASTM International (2012)

ASTM INTERNATIONAL, E1695-95(2013): Standard Test Method for Measurement of Computed Tomography (CT) System Performance, ASTM International (2013)

ASTM INTERNATIONAL, E1814-14: Standard Practice for Computed Tomographic (CT) Examination of Castings, ASTM International (2013)

ASTM INTERNATIONAL, E1935-97(2013): Standard Test Method for Calibrating and Measuring CT Density, ASTM International (2013)

ASTM INTERNATIONAL, E 1931-09 Standard Guide for X rayCompton Scatter Tomography, ASTM International (2009)

ASTM INTERNATIONAL, E1742/E1742M-12 Standard Practice for Radiographic Examination, Book of Standards Volume 03.03, ASTM International (2012)

ASTM INTERNATIONAL, E2002-98(2009) Standard Practice for Determining Total Image Unsharpness in Radiology, Book of Standards Volume 03.03, ASTM International (2012)

ASTM INTERNATIONAL, E2007-00 Standard guide for computed radiology (Photostimulable Luminescence (PSL) Method), Book of Standards Volume 03.03, ASTM International (2012)

ASTM INTERNATIONAL, E2033-99 Standard practice for computed radiology, Book of Standards Volume 03.03 ASTM International (2012)

ASTM INTERNATIONAL, E2597-07e1 Standard Practice for Manufacturing Characterization of Digital Detector Arrays, Book of Standards Volume 03.03, ASTM International (2012)

ASTM INTERNATIONAL, E2698-10 Standard Practice for Radiological Examination Using Digital Detector Arrays, Book of Standards Volume 03.03, ASTM International (2012)

ASTM INTERNATIONAL, E2736-10 Standard Guide for Digital Detector Array Radiology, Book of Standards Volume 03.03, ASTM International (2012)

ASTM INTERNATIONAL, E2737-10 Standard Practice for Digital Detector Array Performance Evaluation and Long-Term Stability, Book of Standards Volume 03.03, ASTM International (2012)

BARRETT H. and SWINDELL W., Radiological Imaging, Vol. 2, Academic Press, New York, NY (1981)

BE, Shan Chiang, GAUTAM S. R., HOPKINS F. F., and MORGAN I. L., "Spatial resolution in industrial tomography", IEEE Trans Nuclear Science, Vol. NS-30, Issue. 2, pp. 1671-30, 2 (1983)

BESSON G., "CT image reconstruction from fan-parallel data", Med. Phys., Vol. 26, pp. 415-426 (1999)

BOONE, J. M., SSIBERT, J. A., "An analytical edge spread function model for computer fitting and subsequent calculation of the LSF and MTF", Med. Phys., Vol. 21, Issue 10, pp. 1541-1545 (1994)

CARL W. E. and VAN EJIK, "Inorganic scintillators in medical imaging", Phys. Med. Biol., Vol. 47, pp. R85-R106 (2002)

CARLSON Carl A., "Imaging modalities in X ray computerized tomography and in select volume tomography", Phys. Med. Biol., Vol. 44, pp. R23-R56 (1999)

CASAGRANDE, J.M., KOCH, A., MUNIER, B., DE GROOT, P., "High Resolution Digital Flat-Panel X ray Detector — Performance and NDT Application", 15th World Conference on Non-Destructive Testing, Rome (2000), http://www.ndt.net/article/wcndt00/papers/idn615/idn615.htm

CHARLTON J. S. (ed.), "Radioisotope techniques for problem-solving in industrial process plants", Leonard Hill, Glasgow & London (1986)

DROEGE, R. T. and MORIN R. L., "A practical method to measure the MTF of CT scanners", Med. Phys., Vol. 9, Issue 5, pp 758-760 (1982)

NEUSER E., SUPPES A., "Computed Tomography & 3D Metrology -Application of the VDI/VDE Directive 2630 and Optimization of the CT System", 11th European Conference on Non-Destructive Testing (ECNDT 2014), October 6-10, 2014, Prague, Czech Republic

EUROPEAN COMMITTEE FOR STANDARDIZATION, EN 444:1994, Non-destructive testing — General principles for radiographic examination of metallic materials by X- and gamma-rays, CEN (2004)

EUROPEAN COMMITTEE FOR STANDARDIZATION, EN 13068-3:2001, Non-destructive testing — Radioscopic testing; Part 3: General principles of radioscopic testing of metallic materials by X- and gamma rays, CEN (2001)

EUROPEAN COMMITTEE FOR STANDARDIZATION, EN 16016-1:2011, Non-Destructive testing — Radiation methods- Computed tomography; Part 1: Terminology, CEN (2011)

EUROPEAN COMMITTEE FOR STANDARDIZATION, EN 16016-2:2011, Non-destructive testing — Radiation methods- Computed tomography; Part 2: Principle, equipment and samples, CEN (2011)

EWERT U., et al., Digital Laminography, Materialforschung **37** 6 (1995) 218–222

EWERT U., et al., New compensation principles for enhanced image quality in industrial radiology with digital detector arrays, Materials Evaluation **68** (2010) 163–168

EWERT., et al., "Strategies for film replacement in radiography — Film and digital detectors in comparison", 17th World Conference on Non-destructive Testing, Shanghai, China, 2008, International Committee of NDT (2008)

EWERT, U., ZSCHERPEL, U., Proceedings of the NAARRI International Conference on Applications of Radioisotopes and Radiation Technology in the 21st Century (2001) 1–17

EWERT, U., Zscherpel, U., "Minimum Requirements for Digital Radiography Equipment and Measurement Procedures by Different Industries and Standard Organizations", Proc. ECNDT 2014, 11th European Conference on Non-Destructive Testing (ECNDT 2014), October 6-10, 2014, Prague, Czech Republic

GRODZINS L., "Optimum energies of X ray transmission tomography of small samples", Nucl. Instrum. Methods Phys. Res., Vol. 206, pp. 541 (1983)

HERMAN G. T., Image Reconstruction from projections, Academic Press, New York (1980)

HILLS A., "Practical guidebook for radioisotope-based technology in industry", IAEA/RAS/8/078, IAEA, Vienna (1999)

HOPKINS, F. F., MORGAN, I. L., ELLINGER, H. D., KLINKSIEK, R. V., MEYER, G. A., AND NEILS, THOMPSON J., "Industrial tomography applications", IEEE Trans. Nuclear Science, Vol. NS-28, Issue. 2, pp. 1717-28, 2 (1981)

HUBBELL J. H., "Photon mass attenuation and energy-absorption coefficients from 1 keV to 20 MeV", Int. J. Appl. Radiat. Isot., Vol. 33, pp. 1269-1289 (1982)

INTERNATIONAL ATOMIC ENERGY AGENCY (IAEA) Safety Standard Series No. SSG-11, Radiation safety in Industrial Radiography, IAEA, Vienna (2011)

INTERNATIONAL ORGANIZATION FOR STANDARDIZATION, ISO 15708-1:2002, Non-destructive testing — Radiation methods — Computed tomography —Part 1: Principles, ISO (2012)

INTERNATIONAL ORGANIZATION FOR STANDARDIZATION, ISO 15708-2:2002, Non-destructive testing - Radiation methods - Computed tomography - Part 2: Examination practices, ISO (2012)

JAMES J.J., DAVIS A.G., COWEN A. R., O'CONNOR P.J., "Developments in digital radiography: an equipment update", Eur. Radiol., Vol. 11, pp 2616-2626 (2001)

JUDY P. F., "Line-Spread Function and Modulus Transfer Function of a Computed Tomographic Scanner", Med. Phys., Vol. 3, No. 4, pp. 233-236 (1976)

KNOLL GLENN. F., “Radiation detection and measurement”, 3rd ed., John Wiley and Sons., New York. (2000)

LELIVELD, C. J., MAAS, J. G., VAN EIJK, C. W. E., and BOM, V. R., "On the significance of scattered radiation in industrial X raycomputerized tomographic imaging", IEEE Trans. Nuclear Science, Vol. 41, Issue. 1, pt.2, pp. 290-294 (1994)

METALS HANDBOOK NINTH EDITION, Vol. 17, Non-destructive evaluation and quality control, ASM International, Metals park, OH 44073 (1989)

NATTERER F., The mathematics of computerized tomography, Wiley, New York (1986)

NICKOLOFF, E. L. and Riley, R., ‘A simplified approach for modulation transfer function determination in computed tomography’, Med. Phys., Vol. 12, Issue 4, pp 437-442 (1985)

PARKER Dennis L., “Optimal short scan convolution reconstruction for fan beam CT”, Med. Phys., Vol. 9, Issue 2., pp. 254-257 (1982)

PERSSON, S. and OSTMAN, E., "Use of computed tomography in nondestructive testing of polymeric materials", Applied Optics, Vol. 24, Issue 23, pp. 4095-4104 (1985)

RAVEN CARSTEN, “Numerical removal of ring artefacts in microtomography”, Rev. Sci. Instrum, Volume 69, No. 8, pp. 2978-2980 (1998)

REIMERS, P., KETTSCHAU, A., GOEBBELS, J., Region-of-interest (ROI) mode in industrial X ray computed tomography, NDT International 23 (1990) 255–261.

RIESEMEIER, H., GOEBBELS, J., ILLERHAUS, B., “Development and application of cone beam tomography for materials research”, Proc. Int. Symp. Computerized Tomography for Industrial Applications, Berlin, 1994, Deutsche Gesellschaft für Zerstörungsfreie Prüfung e.V (DGZFP) (1994) 44:112–119.

SEMENOV SY, SVENSON RH, BULYSHEV AE, SOUVOROV AE, NAZAROV AG, SIZOV YE, PAVLOVSKY AV, BORISOV VY, VOINOV BA, SIMONOVA GI, STAROSTIN AN, POSUKH VG, TATSIS GP, BARANOV VY, “Three-dimensional microwave tomography: experimental prototype of the system and vector born reconstruction method”, IEEE Trans Biomed Eng, Vol. 46, pp. 937-946 (1999)

TANG X., NING R., YU. R., CONOVER D., “Cone beam volume CT image artefacts caused by defective cells in X rayflat panel imagers and the artifact removal using a wavelet analysis based algorithm”, Med. Phys. Vol. 28(5), pp. 812 (2001)

UMESH KUMAR, G. S. RAMAKRISHNA, S. S. DATTA AND V. R. RAVINDRAN, “Prototype gamma-ray computed tomographic imaging system for industrial applications”, Insight (The British Journal of NDT), Vol. 42, No. 10, pp. 662-666 (2000)

UMESH KUMAR, S. S. DATTA, V. R. RAVINDRAN, “3D tomographic visualization of an aluminium manifold specimen on experimental gamma-ray tomographic imaging system”, Proc. 10th APCNDT, Brisbane, Australia. Sep. 17-21 (2001)

UMESH KUMAR, “Simulation of digital radiographic and CT imaging of a mathematically-defined phantom”, Insight (The British Journal of NDT), Vol. 44, No. 1, pp. 40-46 (2002a)

UMESH KUMAR, Planar and volume tomography imaging for NDE applications, BARC Newsletter, Issue No. 309, October 2009 (2009)

VAN EIJK CAREL W. E., “Inorganic-scintillator development”, Nucl. Instrum. Meth. A, Vol. 460, pp. 1-14 (2001)

VAN GRIEKEN R.E., MARKOWICZ A.A. (Eds.), Handbook of X raySpectrometry, Methods & Techniques, Vol. 1–6, Marcel Dekker Inc., New York (1993).

XCOM: Online Photon cross sections database, NIST Standard Reference Database 8 (XGAM), NIST, USA.

ZSCHERPEL, U., et al., “Comparative analysis of radiological detector systems”, 8th ECNDT, Barcelona, 2002, Vol. 1, No. 12, NDT.net (2002)

ZSCHERPEL, U., et al., “Possibilities and limits of digital industrial radiology - The new high contrast sensitivity technique —Examples and system theoretical analysis”, Int. Symp. Digital Industrial Radiology and Computed Tomography, Lyon, France, (2007)

ZSCHERPEL, U., WALTER, D., REDMER, B., EWERT, U., ULLBERG, C., WEBER, N., PANTSAR, T., “Digital Radiology with Photon Counting Detectors”, Proc. ECNDT 2014, 11th European Conference on Non-Destructive Testing (ECNDT 2014), October 6-10, 2014, Prague, Czech Republic

Important Note

In preparation of the present guidebook, many published scientific and technical literatures, reference materials, books and web resources have been the source of relevant information. All experimental gamma or X ray based industrial tomography scanners shown herein for teaching, training and other educational purposes may not be available now. All trademarks, logos and copyrights if cited belong to their respective owners and holders.

IAEA
International Atomic Energy Agency

No. 26

ORDERING LOCALLY

IAEA priced publications may be purchased from the sources listed below or from major local booksellers.

Orders for unpriced publications should be made directly to the IAEA. The contact details are given at the end of this list.

NORTH AMERICA

Bernan / Rowman & Littlefield

15250 NBN Way, Blue Ridge Summit, PA 17214, USA
Telephone: +1 800 462 6420 • Fax: +1 800 338 4550

Email: orders@rowman.com • Web site: www.rowman.com/bernan

REST OF WORLD

Please contact your preferred local supplier, or our lead distributor:

Eurospan Group

Gray's Inn House
127 Clerkenwell Road
London EC1R 5DB
United Kingdom

Trade orders and enquiries:

Telephone: +44 (0)176 760 4972 • Fax: +44 (0)176 760 1640
Email: eurospan@turpin-distribution.com

Individual orders:

www.eurospanbookstore.com/iaea

For further information:

Telephone: +44 (0)207 240 0856 • Fax: +44 (0)207 379 0609
Email: info@eurospangroup.com • Web site: www.eurospangroup.com

Orders for both priced and unpriced publications may be addressed directly to:

Marketing and Sales Unit
International Atomic Energy Agency
Vienna International Centre, PO Box 100, 1400 Vienna, Austria
Telephone: +43 1 2600 22529 or 22530 • Fax: +43 1 26007 22529
Email: sales.publications@iaea.org • Web site: www.iaea.org/publications

International Atomic Energy Agency
Vienna